

University of Windsor

Scholarship at UWindor

Electronic Theses and Dissertations

Theses, Dissertations, and Major Papers

1-1-1976

Design of a partially conducting polymer insulator for outdoor H.V. operation.

A.M-S. Katahoire
University of Windsor

Follow this and additional works at: <https://scholar.uwindsor.ca/etd>

Recommended Citation

Katahoire, A.M-S., "Design of a partially conducting polymer insulator for outdoor H.V. operation." (1976).
Electronic Theses and Dissertations. 6648.
<https://scholar.uwindsor.ca/etd/6648>

This online database contains the full-text of PhD dissertations and Masters' theses of University of Windsor students from 1954 forward. These documents are made available for personal study and research purposes only, in accordance with the Canadian Copyright Act and the Creative Commons license—CC BY-NC-ND (Attribution, Non-Commercial, No Derivative Works). Under this license, works must always be attributed to the copyright holder (original author), cannot be used for any commercial purposes, and may not be altered. Any other use would require the permission of the copyright holder. Students may inquire about withdrawing their dissertation and/or thesis from this database. For additional inquiries, please contact the repository administrator via email (scholarship@uwindsor.ca) or by telephone at 519-253-3000ext. 3208.

DESIGN OF A PARTIALLY
CONDUCTING POLYMER INSULATOR
FOR OUTDOOR H.V. OPERATION

by

A.M-S. KATAHOIRE

A Thesis
submitted to the Faculty of Graduate Studies
through the Department of
Electrical Engineering in Partial Fulfillment
of the requirements for the Degree
of Master of Applied Science at
The University of Windsor

Windsor, Ontario, Canada

1976

UMI Number: EC53138

INFORMATION TO USERS

The quality of this reproduction is dependent upon the quality of the copy submitted. Broken or indistinct print, colored or poor quality illustrations and photographs, print bleed-through, substandard margins, and improper alignment can adversely affect reproduction.

In the unlikely event that the author did not send a complete manuscript and there are missing pages, these will be noted. Also, if unauthorized copyright material had to be removed, a note will indicate the deletion.

UMI[®]

UMI Microform EC53138

Copyright 2009 by ProQuest LLC.

All rights reserved. This microform edition is protected against unauthorized copying under Title 17, United States Code.

ProQuest LLC
789 E. Eisenhower Parkway
PO Box 1346
Ann Arbor, MI 48106-1346

HR 1350

© A.M-S. Katahoire 1976
All Rights Reserved

058060

APPROVED BY:

1.

E. Kuffel

2.

W. E. Kuffel

3.

P. H. Kuffel

4.

M. R. Kuffel

5.

A. Kuffel

ABSTRACT

A power-line insulator is designed using non-conventional materials and concepts. The insulator body consists of three regions: an inner core of fibre glass for mechanical strength, a middle region of a dielectric polymer material, and a partially conducting outer region the thickness of which is calculated to give a uniform current density resulting in a uniform voltage distribution on the insulator surface. The heating effect of this current keeps the insulator surface at a temperature slightly above ambient, deterring moisture condensation.

The insulator geometry is designed to take full advantage of the natural cleansing action of wind and rain while at the same time avoiding the problems associated with these agents. Thus with this design the problem of insulator flashover due to pollution is minimised considerably.

The Finite Element method is used to analyse the field distribution of the insulator design and a comparison with the Finite Difference method of Successive Over-relaxation is made.

ACKNOWLEDGEMENTS

The author wishes to express his gratitude to his supervisor, Dr. E. Kuffel, for the invaluable counselling, guidance and encouragement. Consultations with other Faculty members, especially Dr. M.R. Raghuveer, Prof. P.H. Alexander, and Prof. M.C. Perz, are gratefully acknowledged.

Financial support from the Canadian Commonwealth Scholarship and Fellowship Committee awarded through the author's home (Uganda) government is gratefully acknowledged together with the Canadian Electrical Association who financed the research project.

Mrs. Donna Farquharson deserves thanks for her excellent typing.

TABLE OF CONTENTS

	Page
ABSTRACT	iii
ACKNOWLEDGEMENTS	iv
LIST OF ILLUSTRATIONS	vii
LIST OF TABLES	ix
LIST OF APPENDICES	x
CHAPTER I INTRODUCTION	
1.1 History of the Conventional Power-line Insulator	2
1.2 Format of the Dissertation	10
CHAPTER II POWER-LINE INSULATORS IN A POLLUTED ENVIRONMENT	
2.1 Causes of Pollution	11
2.2 Insulator Flashover due to Pollution	12
2.3 Remedies for Flashover due to Pollution	17
2.3.1 Live line Washing	17
2.3.2 Insulator Greasing	19
2.3.3 Anti-for Insulator Designs	21
2.3.4 Application of Semi-Conducting Glaze	22
CHAPTER III METHODS FOR ANALYSIS OF THE ELECTRIC FIELD DISTRIBUTION OF INSULATORS	
3.1 Introduction	25
3.2 The Finite Difference Methods	27
3.2.1 Finite-Difference Representation of Laplace's Equation for a Three-dimensional Axisymmetric Field	28
3.2.2 Methods of Solving the Finite Difference Equations	32
3.2.3 Application of the SOR Technique to the field of an infinitely extending region	37
3.3 The Finite Element Method	40
3.3.1 Statement of the Problem	41
3.3.2 Subdividing the Continuum	41
3.3.3 Determination of the Interpolation Function	42
3.3.4 Finding the Element Properties	46
3.3.5 Assembling the Element Properties	50

	Page
3.3.6 Solving the System Equations	51
3.3.7 Additional Computations	52
CHAPTER IV DESIGN OF AN ANTI-POLLUTION INSULATOR	56
4.1 Design Factors	57
4.2 The Present Design	65
4.3 Analysis of the Electric Field of the Insulator Design	72
CHAPTER V DISCUSSION AND CONCLUSION	78
5.1 The Numerical Methods	78
5.2 The Insulator Design	86
5.3 Suggestions for Further Work	82
APPENDIX	83
BIBLIOGRAPHY	97
VITA AUCTORIS	100

LIST OF ILLUSTRATIONS

Figure		Page
1.1	46 kV Pin Insulator	3
1.2	11 kV Suspension Insulator	5
1.3	Leakage Distance and Direct Arc Distance of an Insulator	8
1.4	11 kV Post Insulator	9
3.1	Assymetrical Star Grid System	31
3.2	SOR Computer Flow Chart	35
3.3	Equipotential Lines for a Rectangular Trough	36
3.4	Frustrum Subdivided into Element	43
3.5	Equipotential Lines for the Frustrum	53
3.6	Elemental Stress in the Frustrum	54
4.1	Flow of Air Past Insulator Under Surface	60
4.2	Extent of Naturally-Cleansed Surfaces as affected by Number and Shape of Sheds	61
4.3	33 kV Post Insulator	67
4.4	Geometry of the Insulator Design	69
4.5	The Insulator Design	71
4.6	Insulator Subdivided into Elements	73
4.7	Equipotential Lines for the Insulator	74
4.8	Insulator Subdivided into Elements with HV Electrode Reshaped	76
4.9	Equipotential Lines for Insulator with Modified HV Electrodes	77
B3.7	Three Node Triangular Element	85

Figure		Page
D2.1	The Effect of y , number of discharges, insulator diameter, on E_c	95
D2.2	Conventional Anti-fog Insulators	96

LIST OF TABLES

	Page
Table 4.1	66

LIST OF APPENDICES

		page
Appendix A	The Finite Difference SOR Computer Program	83
Appendix B	Determination of a Linear Interpolation Function	85
Appendix C	The Finite Element Method Computer Programs	88
Appendix D		95

CHAPTER I

INTRODUCTION

A power line-insulator is a device intended to give flexible or rigid mechanical support to electric conductors and to insulate these conductors which are at high electric potential from ground. An insulator comprises one or more insulating parts to which connecting devices, metal fittings, are permanently attached and act as electrodes. The electric conductors so supported are part of a transmission line transmitting electrical energy from generating plants to points of utilization.

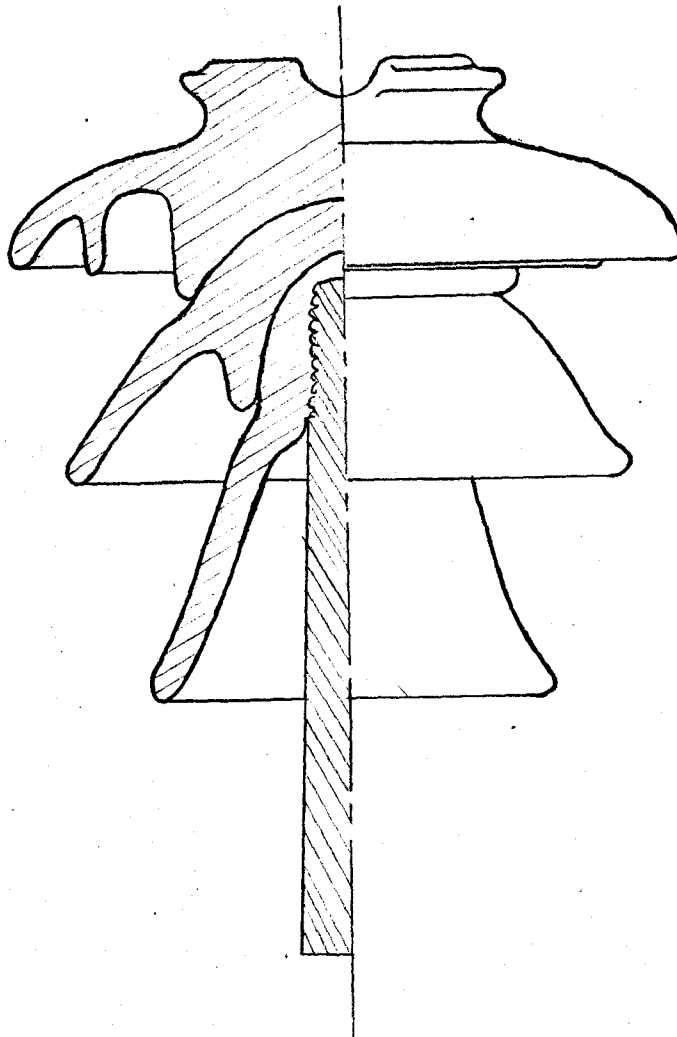
A reliable operating performance, or reliability, of a transmission line depends largely on its insulation. Thus, the fundamental electrical requirement of insulator design is that insulator flashover should not be accompanied by the formation of a conducting path on the surface. Also an ample margin of safety should be provided against puncture. These requirements must be obtained, in so far as possible against any form of lightning-voltage wave, surge frequency or climatic conditions and should be maintained even after the destruction of the more fragile parts of the insulator. Mechanically the insulator must not only have sufficient strength to support the greatest loads of ice and wind that may be reasonably expected, with an ample margin, but be so designed as to withstand

severe mechanical abuse, lightning, and power arcs without dropping the conductor.¹

Porcelain is the most widely used material in the manufacture of power-line insulators. It is a ceramic product obtained by the high-temperature vitrification of clay, finely ground feldspar and silica. It must be free from laminations, pores, and cooling stress, and must be impervious to gasses and liquids to give a high-grade dielectric for high voltage insulators. A smooth surface is obtained by coating the porcelain insulator with a thin film of coloured glass known as glaze. Porcelain has a dielectric strength of 12 - 28 kV/mm, a mechanical strength of 275 MN/m^2 in compression and 20 MN/m^2 in tension. Glass which has undergone a toughening process is the second most used material. It has a dielectric strength of the order of 120 kV/mm and mechanically stronger than porcelain only in compression.²

1.1 History of the conventional power-line insulator

Manufacture of power line insulators began with the advent of transmission of electrical energy by over-head conductors. On this continent this happened during the last decade of the last century. At that time the insulators were made of porcelain and were pin-type (see Fig. 1.1), both single piece and multi-part cemented types. The insulators were more like porcelain cups



$13\frac{1}{2}$ inches diameter

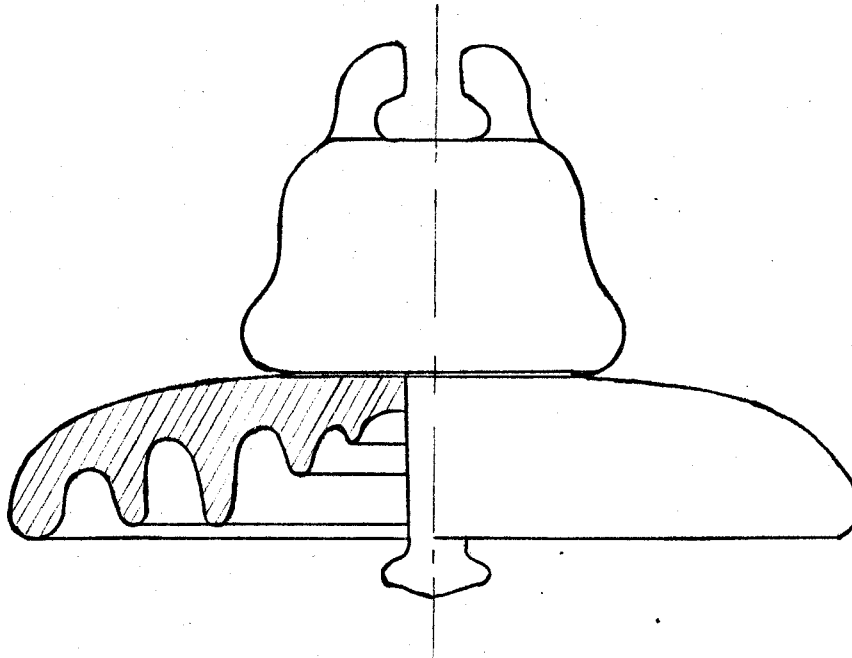
$12\frac{1}{2}$ inches height

Fig. 1.1 46 kV Pin Insulator

cemented together, with but slight understanding of the electric stresses, mechanical and thermal loadings. As a result, with increasing voltages came an increasing amount of insulator trouble until transmission voltage passed the 30 kV mark, during the first decade of this century, when outages due to insulator failures occurred at a rate that for a time threatened the success of high voltage transmission of electric energy.^{3, 4}

Lack of previous operating experience resulted in many designs as suggested remedies, with none based on a rational study of the insulator as a direct problem; besides the properties of porcelain were not known as we understand them today. Consequently insulators were manufactured with flashover distances larger than warranted by the thickness of the porcelain resulting in puncture.

The second decade of this century marked a great deal of improvement in porcelain, cement and the electrical properties of the insulator. However, the increasing size of the pin insulator with increasing system voltages reached an economical limit at 66 kV. The suspension insulator, Fig. 1.2, overcame this economical problem. With increased voltages came the problem of flashover due to contamination or pollution of the insulator surface. By the 1930's both pin and suspension insulators had reached a marked degree of reliability in service. This was due



10 inches diameter
5 ³/₄ inches height

Fig. 1.2 11 kV Suspension Insulator

to designing with adequate factors of safety and better understanding of the insulator problem. The following considerations were necessary for higher reliability:

a) Allowance for cubical expansion under temperature changes. Otherwise if the three materials porcelain, cement and steel were tightly compressed in an unyielding manner enormous stresses under temperature changes would result due to their widely different coefficients of cubical expansion.

b) Avoidance of electrical puncture due to lightning and power arcs. Insulators were to be designed such that parts would be apportioned to insure uniform distribution of stress and the thickness would be gradually increased from the edge of the shed inwards to the stem and porcelain was to be of high thermal capacity. An electrical factor of safety in service was introduced as a design criterion. It is the ratio of puncture voltage to the product of power line frequency (60 Hz) flashover voltage and the impulse ratio. The impulse ratio is the ratio of insulator flashover at high frequency to flashover at normal power line frequency. The impulse ratio was required to be at least three.

c) Damage by mechanical overloading and impact shocks. Impact shocks arose from bullet shots (insulators made a good target for irresponsible marksmen). To avoid damage, insulators were made of thicker material and ample margin

of safe operation during the most severe loading conditions.

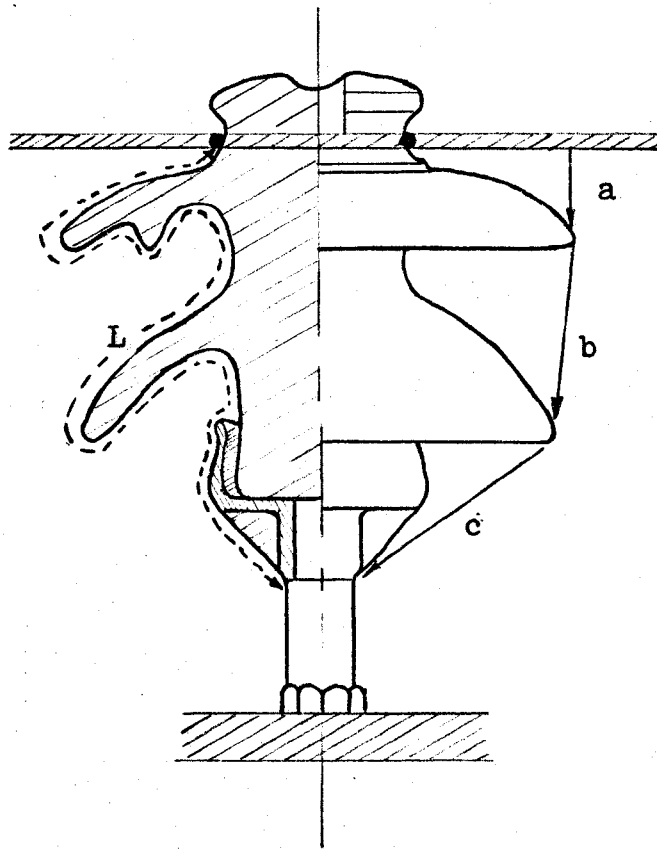
d) Avoidance of porosity in the insulator material. The thicker the porcelain the more necessary it was found to improve the soundness of the material, thus further improvement in porcelain and glass continued.

e) High leakage current leading to flashover. Defined as the current flowing through an electrical insulating system to ground, the leakage current was found to increase during adverse climatic conditions with heavy contamination or pollution on the insulator surface resulting in surges and flashover. Longer leakage path length (see Fig. 1.3)

with as much of it as possible kept dry, resulted in insulators of better performance. The need for adequate leakage path length resulted in the introduction of corrugations, ribs or skirts in the undersurface of suspension insulators. The dry flashover of an assembled insulator was required to be three to five times the nominal operating voltage and the leakage distance to be at least twice the shortest air-gap distance, (see Fig. 1.3.)

f) Corona discharges at potentials much below the flash-over voltage in pin-type insulators. Semi-conducting glaze was applied at the head of the pin insulator to ensure proper contact between the conductor, tie wire and the porcelain.⁴

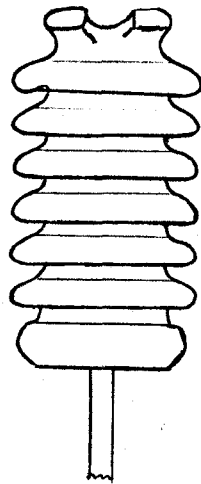
The post insulator, Fig. 1.4, was introduced in the



L - Leakage Distance

a + b + c + - Direct Arc Distance

Fig. 1.3 Leakage Distance & Direct Arc
Distance of an Insulator



6 inches diameter

11½ inches height

Fig. 1.4 11kV Post Insulator

early forties to overcome the radio interference problem associated with the pin-type insulator. Post insulators are both line and apparatus insulators.

1.2 Format of the Dissertation

Increased voltages have resulted in more outages due to insulator flashover due to pollution on the insulator surface and other agents. Remedies for flashover due to pollution have not been successful in eliminating this problem; thus there is a clear need for better remedies. This work aims at reducing the pollution problem.

A literature survey was carried out to establish the state of the art in power line insulators and their flashover due to pollution. Chapter II gives the causes and consequences of pollution, remedies and their limitations in applications for flashover due to pollution. Chapter IV gives the design criteria or value system for the design of a power line insulator for a polluted environment. Subsequently the design procedure is given, and then the electric field analysis of the designed insulator using numerical methods developed in Chapter III. Discussion of results, conclusions and suggestions for further work are given in Chapter V.

CHAPTER II

POWER LINE-INSULATORS IN A POLLUTED ENVIRONMENT

2.1 Causes of Pollution

The pollution in industrial areas may be extremely varied, depending on the origin of the dust and its concentration in the atmosphere, in addition to meteorological conditions. Pollution deposit ('industrial dirt') has the following composition: soot, tar, oil (these form an adhesive base) and mineral dusts mainly, of the oxides of silica, iron, calcium and magnesium, which form a conducting or electrolytic paste on the surface of the insulator when wetted. The wetting agents include dew, drizzle and fog. For example, on insulators operating in the vicinity of cement works, little deposit usually gathers on the upper surface, as the fine cement dust is cleaned off by wind and rain, while a large quantity collects between the corrugations on the underside of the insulator. Moistening of the pollution on the underside results in a porous mass, which is baked hard by the heat generated by the heavy surface-leakage currents, becoming so hard that only chipping can remove the mass. Generally, industrial dirt is windborn: its composition depends on the chemical processes inherent in the nature of the industrial activity. Other industrial pollution sources include coke-ovens, brick works, power stations and chemical works.

Locomotives, smouldering pit-heaps and collieries constitute sources for smoke, dust and coal dust contamination.

In coastal areas, the fouling of insulators is due to the settling of salt and salty compounds on the insulator surface. The salt contamination is born by spray carried by a strong wind blowing off the sea.

In deserts or conditions of extreme drought, windborn dust is electrostatically attracted to the insulator underside, especially in the region near the pin, eventually bridging the gaps and causing sparks in the overstressed air.^{5,6}

2.2 Insulator Flashover due to Pollution

When the pollution deposit on the surface of an insulator is dry, its performance remains practically unaffected. However, if the soluble constituents of the contamination on the insulator surface become moist, an electrolytic film is formed greatly distorting the electric field along the insulator, which becomes unstable and can lead to flashover. Whether a complete flashover or only corona, or streamer, discharge will follow will depend on the amounts of deposit and moisture on the insulator surface, on the insulator shape and on the meteorological conditions surrounding the insulator and on the voltage across the insulator. Streamers occur at points of maximum stress; if the surrounding air is dry, ionic winds result in eddy currents of air. Under moist conditions, the effect is the

circulation of a maximum amount of dirt-laden moist air in the insulator undersurface, especially around corrugations. Meteorological conditions which enhance streamers followed by flashover include a combination of a long dry period with heavy pollution, preceding mist or a period of fog with freezing temperatures subsequently followed by a thaw. A combination of fog and frost, or melting snow blown^a onto soiled insulator in high wind, may give rise to very severe surging.⁷⁻¹⁰

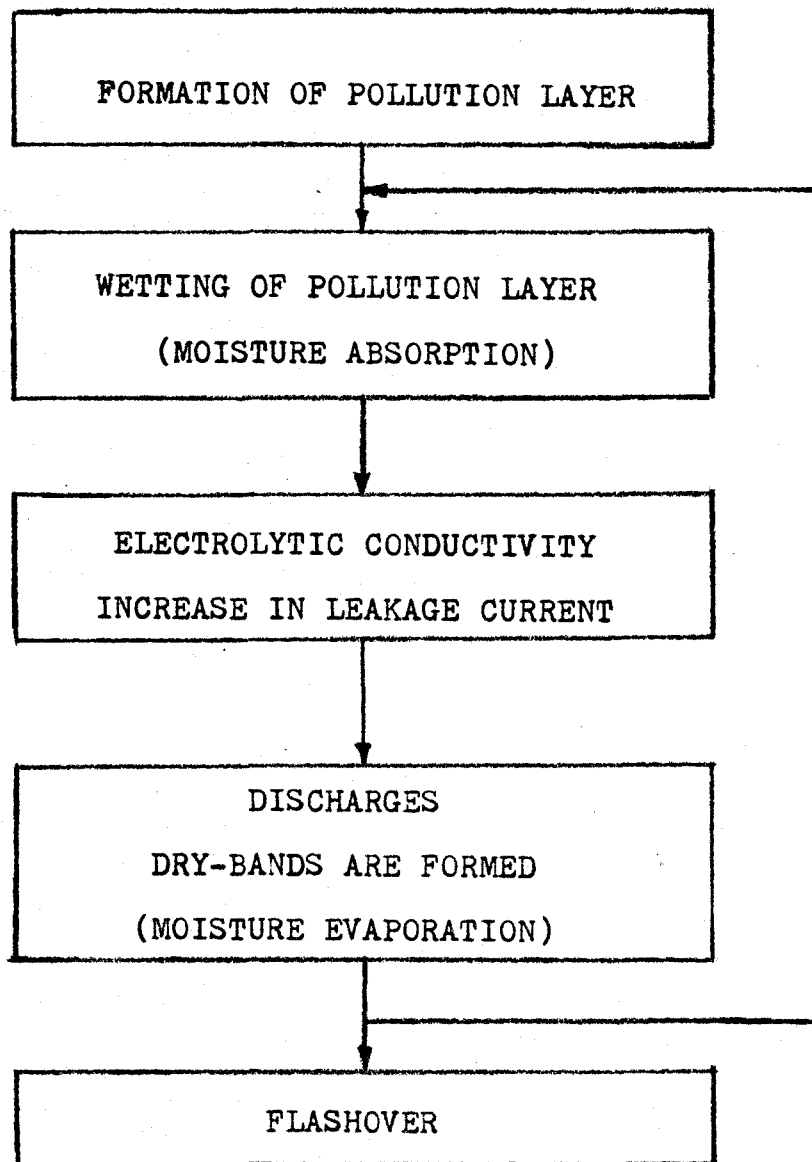
The stress resulting from the distortion of the electric field on the surface of the contaminated insulator may cause visible discharge at the metal cap at a voltage equivalent to fifty percent of the wet flashover value. The local stress may then exceed the electric strength of air; sparkover will occur causing discharges along small portions of the insulator. These discharges are maintained by current flowing through discharge-free, but polluted, portions of the insulator surface.

Owing to the heat generated at the discharge roots, the pollution dries out in their neighbourhood and ceases to conduct. The dry, but contaminated, portions of the insulator so formed are called "dry-bands". To maintain conduction, the discharge root must travel along the surface to a region which is still moist. In other words, the leakage current, which has a variable density and is therefore highest at the narrowest parts of the insulator, must

increase with incremental charge in the discharge path. The discharge can therefore elongate and complete flash-over will occur if the distance between electrodes is bridged.^{6, 11}

However, these discharges do not necessarily lead to flashover. Polluted insulators often exhibit sparks which are extinguished after spanning only a fraction of the insulator surface. Using experimental models, it has been found that the voltage necessary to maintain a local discharge on a polluted insulator increases with increasing discharge length and, if this voltage exceeds the voltage across the insulator electrodes discharge, extinguishes without flashover.⁶

Dry-bands increase the surface resistance, thus decreasing the leakage current. In consequence, re-absorption of the moisture by the dry deposit and reforming of the electrolytic film on the insulator surface take place. When the rate of moisture absorption exceeds the rate of evaporation, the excessive leakage current will cause ionization of the air in the immediate vicinity of the surface and the resistance of the path of the surge will be reduced, thus increasing the current, until flashover occurs. On the other hand, if the rate of evaporation, the rate of formation of dry-bands, exceeds that of moisture absorption, intermittent discharges occur. These, if in a considerably large number, produce transient voltages the



FLOW CHART FOR INSULATOR FLASHOVER DUE
TO POLLUTION

magnitudes of which may be high enough to cause the insulator to flashover.^{6, 11} A schematic presentation is given on page 15.

Using experimental models¹² with constant surface resistance, r_c ohms per unit cm length, the maximum stress E_c , volts peak per cm, before flashover was found to be related to the pollution resistivity ρ ohm-cm by

$$E_c \propto \rho^{0.43} y^{0.43}$$

where y is the number of surges in parallel on the insulator surface. The constant of proportionality depends on the insulator shape but has a minimum value of $10.5 r_c^{0.43}$ at power frequency. The graph of Fig. 2.1 shows the variation of E_c with y . (The graph of Fig. D2.1 shows the variation of E_c with y . Appendix D). The corresponding

$$I_c = 223/E_c^{1.31} \text{ Amps}$$

Physically, at each stage during the processes that precede flashover the surfaces cleaner and drier than the other parts of the insulator form an obstacle to the leakage current causing an interruption in discharge. If the arcs are divided over the entire surface of the insulator with varying surface resistivity, then the probability that the arcs will line up along the direction of the field is remarkably reduced thus impeding the inception of flashover.¹²

In addition to a possibility of flashover, contamination of insulators leads to non-linear voltage distribution

across an insulator string and the non-linearity increases with increasing the density of pollutants on the surface of insulators. Severe surging results in high power losses and intense radio interference. The switching surge flashover voltage of an insulator assembly is lowered by the presence of contaminants on the surface of an insulator. On the other hand switching surges on polluted insulators can reduce the wet flashover voltage to as low as fifty per cent of the dry flashover value. Presence of dry-bands on polluted insulators causes a further reduction in switching surge flashover voltage. However, to cause these reductions the duration of the surge has to be long -- of the order of 2 ms.^{13, 14}

Artificial laboratory tests have been developed to help in assessing insulator performance in natural conditions. Because of the tremendous statistical variation in the climatic influence to which insulators are exposed, these methods differ as widely as the pollution itself. The Salt Fog Test and the Dust Deposit Test have been accepted by CIGRE as standard anti-pollution tests and are described in reference.¹⁵

2.3 Remedies for Flashover due to Pollution

In live line washing of insulators compressed air and water at desired temperature and of known conductivity are applied using equipment similar to that used for fire fighting. The nozzle is designed to give either a jet

wash or a spray wash, the latter resembles rainfall and is more effective in areas where the pollutant has low adhesive properties or is water soluble otherwise the former is used.

If thick layers of pollution have been allowed to build up, some danger of flashover during the initial stage of the washing exists. Therefore, for safety it is necessary to inspect the state of insulators in order to avoid flashover during washing. Surge counts, records of 25 mA r.m.s. leakage current surges, are used to assess the insulator surface electrical instabilities. Insulator washing is carried out after a certain number of such counts, determined from operational experience. The use of automatic control has reached a stage where automatic pollution detectors indicating the amount of pollution rather than leakage current surges have been installed. However, the need for a periodical hand cleaning of the insulators and checking for water penetration into equipment still remain the direct responsibility of the foreman.¹⁴ Other factors affecting the reliability of the hot line washing remedy include the requirement for maximum conductivity of water related to quantity (2600 to 8000 ohms/cm³), the requirement for optimum water pressure and suitable jet or spray nozzle design (130-150 lbf/sq.in.). Operation in adverse conditions and cost and maintenance are other factors.

2.3.2. Insulator Greasing

The physical principle in the application of coatings on the surface of the insulator lies in the fact that pollution flashover is preceded by the formation of an electrolytic film. Attempts have, therefore, been made to reduce the catching of soluble pollution and to prevent the formation of a continuous film by the use of solids such as P.T.F.E. (Polytetrafluorethylene) which have low coefficients of friction and are water-repellant. The essential common feature of successful greasy coatings is to provide surfaces that are self renewing; the pollution being either smothered by the exuded oil or is bodily engulfed. No ideal coating has yet been found. The coating surface of most materials used is covered by deposits after some time or the materials are degraded by discharges.

Silicone oil or polymer coatings on high voltage insulators showed satisfactory results, however, the life of these coatings was inadequate, and attention was turned to silicone greases applied in thick layers which last only three years. The broad classes of satisfactory material are petroleum jellies, silicone greases, and strippable compounds.

Petroleum jellies include materials made from hydrocarbon oils, slack and microcrystalline slacks. They soften with increase of temperature and melt at the sites of discharges, so engulfing the pollution. On cooling

they resume their former properties. Heating may cause petroleum jellies to slide; this limits their application to temperate climates and precludes their use on some insulators.^{9, 16}

Silicone greases are composed of silica filler and a silicone oil which is the active component. They do not melt, but decompose at temperatures of about 200 C. They may be used in all climates and on hot insulators on account of their substantially constant viscosity (-50°C to 200°C). Apart from their high cost, a further disadvantage is that discharge activity exposes the silica filler, which then acts as a pollutant.

Strippable compounds are blends of waxes, oils and copolymers of ethylene - vinyl - acetate or ethylene - vinyl - acrylate type. During their active life they exude oil both outwards, smothering pollution on their exposed surfaces, and inwards protecting the interface with the insulator surface. They revert to their original state after melting at discharge sites.

Mineral-loaded hydrocarbons and true greases containing metal soaps are other coatings worth mentioning. Possibility of ignition and inability to revert to original properties after melting, respectively, are the causes of their unsatisfactory protection. In all the above cases application of the coating is by hand, deep greasing or spraying. Degreasing is also by hand, heat or vapour from organic

solvents and can be more problematic than greasing.

The major disadvantages of insulator greasing include the need to maintain the grease in good condition and the considerable plant outage time required.^{9, 16}

2.3.3. Anti-fog Insulator Designs

In the early 1930's empirical results were obtained which showed that the suspension cap-and-pin insulators with large vertical and exposed surface under conditions of fog gave the best performance. Accordingly a bell-shaped insulator replaced the then existing disc insulators. Subsequent poor experience with the bell-type insulator led to development of test methods which would establish the optimal shape for insulators for use under conditions of fog. As a result of many attempts to obtain some geometrical criterion which would enable the relative merits of various insulator geometries to be assessed the leakage or creepage path length was chosen as a design factor.

The main aim has been to decrease the leakage current during fog. This was achieved by increasing the leakage path length thus increasing the surface resistance of a polluted insulator. The surface resistance has been found to vary directly with length and inversely as to width of the insulator, and can be represented by the expression:

$$R = K \int_0^s \frac{ds}{b(s)}$$

Where K is the resistance in ohms of a leakage path 1 cm

long 1 cm wide;
s is the total leakage path length and
b(s) is the variable circumference of the insulator geometry.
The integral alone is called the form factor, a parameter
that is difficult to calculate but can be determined
graphically. A very efficient way of increasing the surface
resistance with a small diameter was the introduction of
skirts or deep ribs in the insulator undersurface. Fig.D2.2
shows some anti-fog insulator shapes.

The main disadvantage of the anti-fog insulator is that
corrugations on the underside of the insulator give a larger
surface area for airborne deposits hence a greater surface
area becomes contaminated and remains so even after a
normal rainfall. This results in highly conducting compounds
being formed and greatly depreciating the surface insulation.

2.3.4. Application of Semi-conducting Glaze

The use of resistive glazes on high voltage insulators
to prevent radio interference has been a proven technique
for many years. Glaze was applied around the high voltage
electrode to prevent any large potential differences
building due to lack of contact between the insulating
material at the electrode and the electrode resulting in
local arcing and consequent radio interference.

For the purposes of preventing contamination flashover,
resistive-glazes are applied as a thin film on the surface
of the insulator. A heating current flows through this

film, the heating effect of which raises the insulator surface temperature slightly above ambient. If this is sufficiently high, no moisture condensation will occur on the insulator surface, thus preventing the formation of an electrolytic paste that would result in a high leakage current and hence instabilities on the insulator surface. The resistive-glaze also stabilizes the voltage distribution along the length of the insulator and prevents the formation of the highly-stressed dry-bands by providing a path to the leakage current of lower impedance than one across the dry-bands.

From in-service tests, it has been found that a current of the order of 1 mA should flow through a continuous resistive layer at normal operating voltage so as to effect a surface heat dissipation of at least 0.008 watts per square centimeter, in order to effectively evaporate any kind of condensation on the insulator surface.¹⁷

The advantages of this remedy include prevention of the need for greasing and washing is required at less frequent intervals. The insulator leakage distance is better utilized. It is common practice among the Utilities to use insulators with extra leakage distance so as to be able to extend sufficiently the period between washings, in order to coincide with natural washing of insulators during the wet season. Application of a resistive glaze on insulator surfaces also results in a much better voltage distribution across

a string of insulators.

Earlier ferrite glaze applied to the surface of insulators was found to have a very short life, mainly due to electrolytic corrosion under the influence of applied voltage and moisture. All glazes developed so far have a negative temperature coefficient: Therefore, as a result of the heating effect of the heating current, a danger of thermal runaway exists. Glazes based on tin oxide and antimony oxide system are much more resistant to electrolytic corrosion and have a much lower negative temperature coefficient of resistivity than the ferrite glazes, so that there is much less variation of the stabilizing (heating) current with ambient temperature. Nevertheless, there still exists a danger that if over-voltage occurs or is applied, the insulator temperature will rise, resulting in thermal runaway.¹⁷⁻¹⁹

CHAPTER III

METHODS FOR ANALYSIS OF THE ELECTRIC FIELD DISTRIBUTION OF INSULATORS

3.1 Introduction

Transmission voltages have risen remarkably rapidly in recent years and there is every indication that even further substantial increases are to be expected. The very high voltage levels now becoming common have posed many difficult problems for the equipment designer, especially in connection with insulation. At the same time extensive work has to be devoted to such factors as the effect of pollution on insulators and bushings for better reliability. Therefore a clear need exists for the equipment designers to develop and/or use methods that give accurate results in the analysis of the electric field surrounding high voltage conductors, bushings, insulators and other hardware and for evaluating the effect on performance of such factors as contamination, mechanical damage, etc.

The electrostatic field distribution of the power line equipment is determined by solving Laplace's equation everywhere outside the conducting portions or electrodes.

$$\nabla^2 V = 0 \quad (3.1)$$

where V is the electric scalar potential. The problem is generally not bounded in that V approaches zero value at very great distances from the region of interest. Only

purely analytical methods are capable of dealing with this condition exactly -- at least as of this date. However, analytical solutions of Laplace's equation can only be obtained for relatively simple electrode systems and boundary shapes. Therefore the multiplicity of dielectric interfaces and boundary conditions for the complicated contours encountered in power line equipment means that analytical solutions for potential are not possible. Several approximation methods have been developed, the more important of these being analogue and numerical methods.²⁰

Among the most popular and versatile analogue technique is the electrolytic tank but the difficulty with this technique is that it cannot cope well with the fact that the problem region is unbounded. The technique demands considerable equipment and careful measurements for good results to be obtained. Extension to multidielectric fields is both difficult and prone to error.

Numerical methods of solutions which express the Laplace equation in finite difference form of pointwise approximation have been developed and applied quite extensively. However, the superior finite element methods of piece-wise approximation have only recently been applied to the solution of Laplace's equation for the electric scalar potential V . In the following two sections both methods are developed by case studies, thus emphasizing

their application in real engineering problems rather than giving them a theoretical treatment. The successful use as well as the limitations in the application of both methods to the insulator design is also given.

3.2 The Finite Difference Methods

The solutions obtained by finite difference methods consist of the value, at discrete points regularly spaced over the whole field region, of the function, V , describing the field in the whole problem region. These values are obtained by replacing the one partial differential equation describing the field by many simple finite-difference equations which take the form of linear equations connecting the potential at each point with the potentials at other points close to it. In this way, the solution of the field problem is reduced to the solution of a set of simultaneous equations. Because of the large number of these equations normally occurring, (a consequence of the finite-difference approximation which requires a closely spaced grid for high accuracy) it is not practical in most cases to solve the equations using methods involving determinants, or elimination on account of the excessive computer time and storage requirements.

Relaxation and Iteration are the basic methods used to solve the finite-differences simultaneous equations. Both methods are discussed in a subsequent section together with their modified form used in this work.

Any finite difference method of solving Laplace's equations involves setting up a finite-difference approximation of equation (3.1) and then solving the resulting simultaneous equations subject to the boundary conditions.

3.2.1. Finite-Difference Representation of Laplace's
Equation for a Three-dimensional Axisymmetrical Field

In replacing the field equation by a set of finite-difference equations which relate values of V at discrete points, a regular spatial distribution is used so that the same form of these equations is satisfied at all the points in the solution region. Such regular distributions are given by the geometric arrangement of points lying at the nodes of any regular network, mesh or grid system. In this work a rectangular mesh was used with a coordinate system designated (r, z) for the radial direction and third dimension respectively.

For the case of three dimensions with axisymmetry (no variation of V with rotation about the axis of the third dimension) equation (3.1) becomes

$$\frac{\partial^2 V}{\partial r^2} + \frac{1}{r} \frac{\partial V}{\partial r} + \frac{\partial^2 V}{\partial z^2} = 0 \quad (3.2)$$

The short-hand notation of equation (3.3) is used (see Fig. 3.1)

$$V_{i,j} = V(r,z) \Big|_{z = z_i, r = r_j} \quad (3.3)$$

The finite-difference approximation to equation (3.3) is developed by expanding the potential at all the four nodes $V_{i,j+1}$, $V_{i,j-1}$, $V_{i+1,j}$, $V_{i-1,j}$ about point 0, $V_{i,j}$, of Fig. 3.1, in a Taylor's series to derive expressions for

$$\left. \frac{\partial^2 V}{\partial r^2} \right|_0, \quad \left. \frac{\partial V}{\partial r} \right|_0 \text{ and } \left. \frac{\partial^2 V}{\partial z^2} \right|_0 \text{ which are substituted}$$

into equation (3.3). For the node at (r_{j+1}, z_i) Taylor expansion about node 0 gives

$$V_{i,j+1} = \underline{V_{i,j}} + Q \left. \frac{\partial V}{\partial r} \right|_0 + \frac{1}{2!} Q^2 \left. \frac{\partial^2 V}{\partial r^2} \right|_0 + \frac{1}{3!} Q^3 \left. \frac{\partial^3 V}{\partial r^3} \right|_0 + \dots \quad (3.4)$$

For $V_{i,j-1}$ by a similar expansion about 0 we get

$$V_{i,j-1} = V_{i,j} - W \left. \frac{\partial V}{\partial r} \right|_0 + \frac{1}{2!} W^2 \left. \frac{\partial^2 V}{\partial r^2} \right|_0 - \frac{1}{3!} W^3 \left. \frac{\partial^3 V}{\partial r^3} \right|_0 + \dots \quad (3.5)$$

Multiplying (3.4) by W and (3.5) by Q and adding results in

$$\left. \frac{\partial^2 V}{\partial r^2} \right|_0 = \frac{2V_{i,j+1}}{Q(W+Q)} + \frac{2V_{i,j-1}}{W(W+Q)} - \frac{2V_{i,j}}{WQ} \quad (3.6)$$

after rearranging and neglecting powers of order four and higher in W and/or Q.

Similar operations for nodes at (r_j, z_{i+1}) and (r_j, z_{i-1}) result in

$$\left. \frac{\partial^2 V}{\partial z^2} \right|_0 = \frac{2V_{i+1,j}}{P(P+S)} + \frac{2V_{i-1,j}}{S(P+S)} - \frac{2V_{i,j}}{PS} \quad (3.7)$$

Subtracting equation (3.5) multiplied by Q^2 from equation (3.4) multiplied by W^2 and neglecting third and

higher power terms gives

$$\frac{\partial v}{\partial r} = \frac{W}{Q(W+Q)} V_{i,j+1} - \frac{Q}{W(W+Q)} V_{i,j-1} - \frac{(W-Q)}{WQ} V_{i,j} \quad (3.8)$$

Substituting for equations (3.6), (3.7) and (3.8) and rearranging gives

$$V_{i,j} = \left(V_{i,j+1} \frac{1 + \frac{W}{2R}}{Q(Q+W)} + V_{i,j-1} \frac{1 - \frac{Q}{2R}}{W(W+Q)} + \frac{V_{i+1,j}}{P(P+S)} + \frac{V_{i-1,j}}{S(P+S)} \right) \cdot \frac{1}{\frac{1}{WQ} + \frac{1}{SP} + \frac{W-Q}{2WQR}} \quad (3.9)$$

where $R = r_j$

The simplifying assumptions made in developing (3.9) involve neglecting higher powers in W , Q , S , P , the mesh size parameters, resulting in a truncation error. Practically, the mesh size should be chosen to minimize the truncation error. Application of equation (3.9) to all nodes which lie to the interior of the boundary nodes results in a set of simultaneous equations whose matrix representation would be

$$[M] [V] = [B] \quad (3.10)$$

where M is a sparse matrix of the coefficients of unknown potentials $V_{i,j}$, V is a column matrix of unknown potentials $V_{i,j}$ and B is a column matrix of the sums of the known potentials at the boundary and the source term, where applicable.

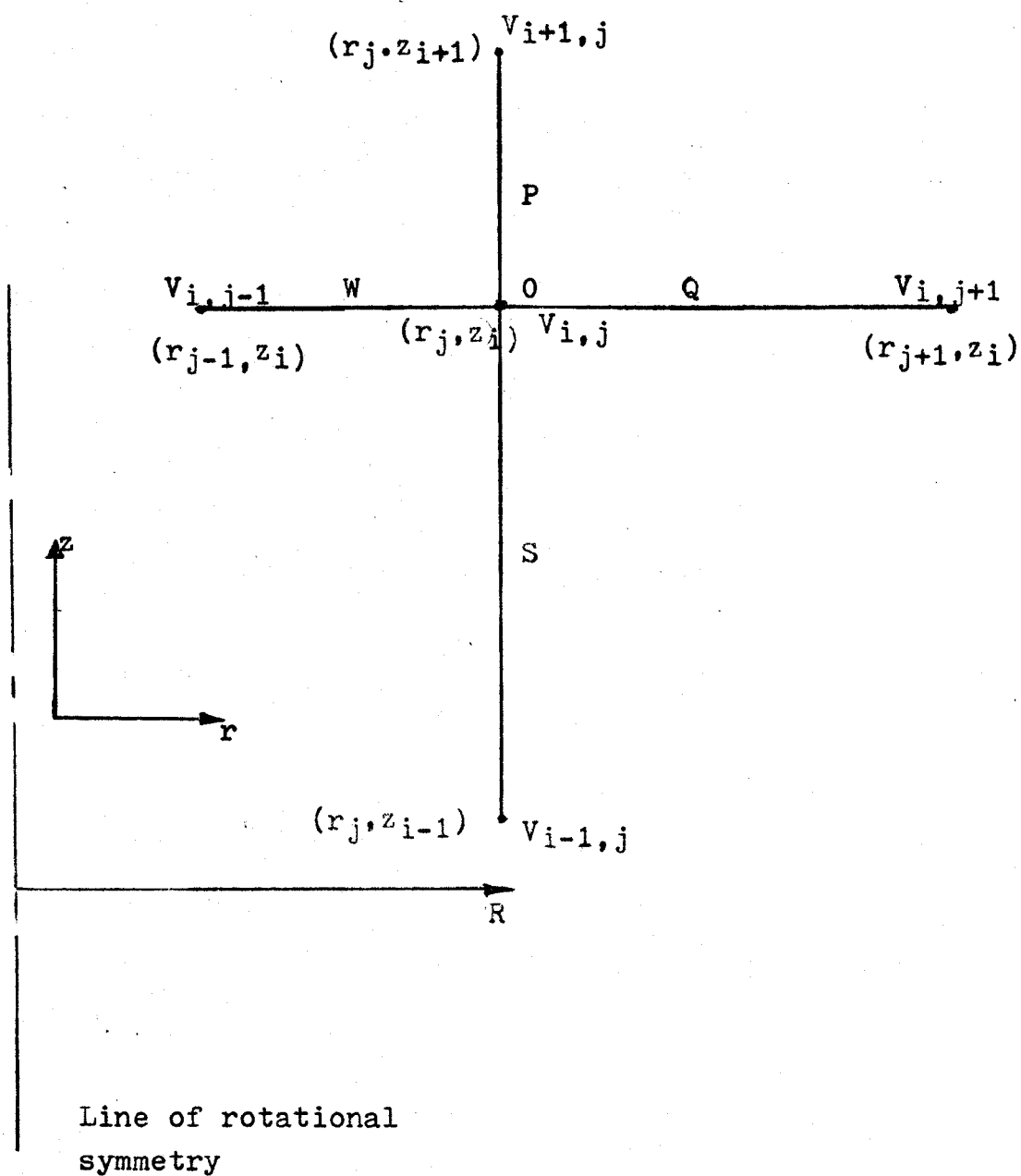


Fig. 3.1 Assymetrical Star Grid System

3.2.2. Methods for solving the Finite Difference Equations

Iteration and relaxation methods are similar except that relaxation developed as a hand computation technique and is therefore more suitable for simple field problems. In iterative methods, improved values of V are determined directly from the difference equation (3.9); each node being considered in turn in a fixed repeated cycle. The designation of each node by (i,j) fully facilitates this iterative computation and the use of a digital computer.. The most highly developed iterative technique for solving the finite-difference simultaneous equations is the Extrapolated Liebman method.^{21,22} The nodes in the solution region are scanned in succession continuously replacing $V_{i,j}$ by an adjusted value starting from an initial assumed set of approximations. The adjusted value is obtained by overrelaxing (altering by too much) each node potential so that the corresponding difference between the exact and the estimated value (known as the residual) of the potential at each node is depressed beyond zero. As the exact solution is approached the amount of overrelaxation in neighbouring nodes will be just right such that recalculation of the potential at a given node will bring the residual at that node back to zero. This technique is known as successive Point Overrelaxation (SOR in short form). SOR improves the convergence rate.

To have a better understanding of the application of

SOR consider as a case study a rectangular trough with a square cross-section area of side 48 inches and with three of the four sides at high voltage and the fourth side grounded. A mesh size of $P = S = W = Q = 1$ was chosen and the gap between the high voltage sides and the grounded side was chosen to contain four nodes excluding the two boundary nodes at high voltage and ground potential. The resulting form of equation (3.9) for this grid system is

$$V_{i,j} = \frac{1}{4} (V_{i+1,j} + V_{i-1,j} + V_{i,j+1} + V_{i,j-1} - 4 * V_{i,j}) \quad (3.11)$$

Applying the SOR technique on node (r_j, z_i) at the $(n+1)^{th}$ iteration, equation (3.11) becomes

$$V_{ij}^{(n+1)} = V_{ij}^{(n)} + \frac{a}{4} \left(V_{i+1,j}^{(n)} + V_{i-1,j}^{(n)} + V_{i,j+1}^{(n)} + V_{i,j-1}^{(n)} - 4 * V_{i,j}^{(n)} \right) \quad (3.12)$$

where a is the convergence factor determining the degree of overrelaxation, and has values between 1 and 2. The value of unity corresponds to the basic iterative technique in which only current approximations to V are stored.

When $a = 2$ the iteration process becomes non-convergent. To take advantage of the SOR technique an optimum value of the convergence factor should be used but its determination causes considerable difficulty.

For a rectangular region of $(m \times n)$ nodes it has been shown²³ that

$$a = 2 \left(1 - \pi \sqrt{\frac{1}{(n-1)^2} + \frac{1}{(m-1)^2}} \right)$$

and

$$a = 2 \left/ \left(1 + \sin \frac{\pi}{(m-1)} \right) \right. \quad (3.13)$$

for a square region with m nodes on a side. In both cases, however, equations (3.13) only hold for Dirichlet problems (values of V initially specified at the boundary); empirical determination of a is thus necessary in almost all other cases.

A computer flow chart for application of the SOR technique for the rectangular trough is given in Fig. 3.2. Symmetry exists between two halves of the region of interest and thus the problem was only solved for half the cross-sectional area. For node (i,j) at the line of symmetry equation (3.12) was modified such that the term $V_{i,j+1}$ was replaced by $V_{i,j-1}$ on account of symmetry. Equation (3.12) thus becomes

$$v_{i,j}^{(n+1)} = v_{i,j}^{(n)} + \frac{a}{4} \left(v_{i+1,j}^{(n)} + v_{i-1,j}^{(n)} + 2 v_{i,j-1}^{(n)} - 4 v_{i,j}^{(n)} \right) \quad (3.14)$$

The computer program which implements this calculation is given in Appendix A and the plotted results are shown in Fig. 3.3. The computer time required for (49×25) nodes to reduce the maximum absolute value of the residual to 0.01 per cent including time for sorting and plotting was just over half a minute, the optimum convergence factor being 1.707.

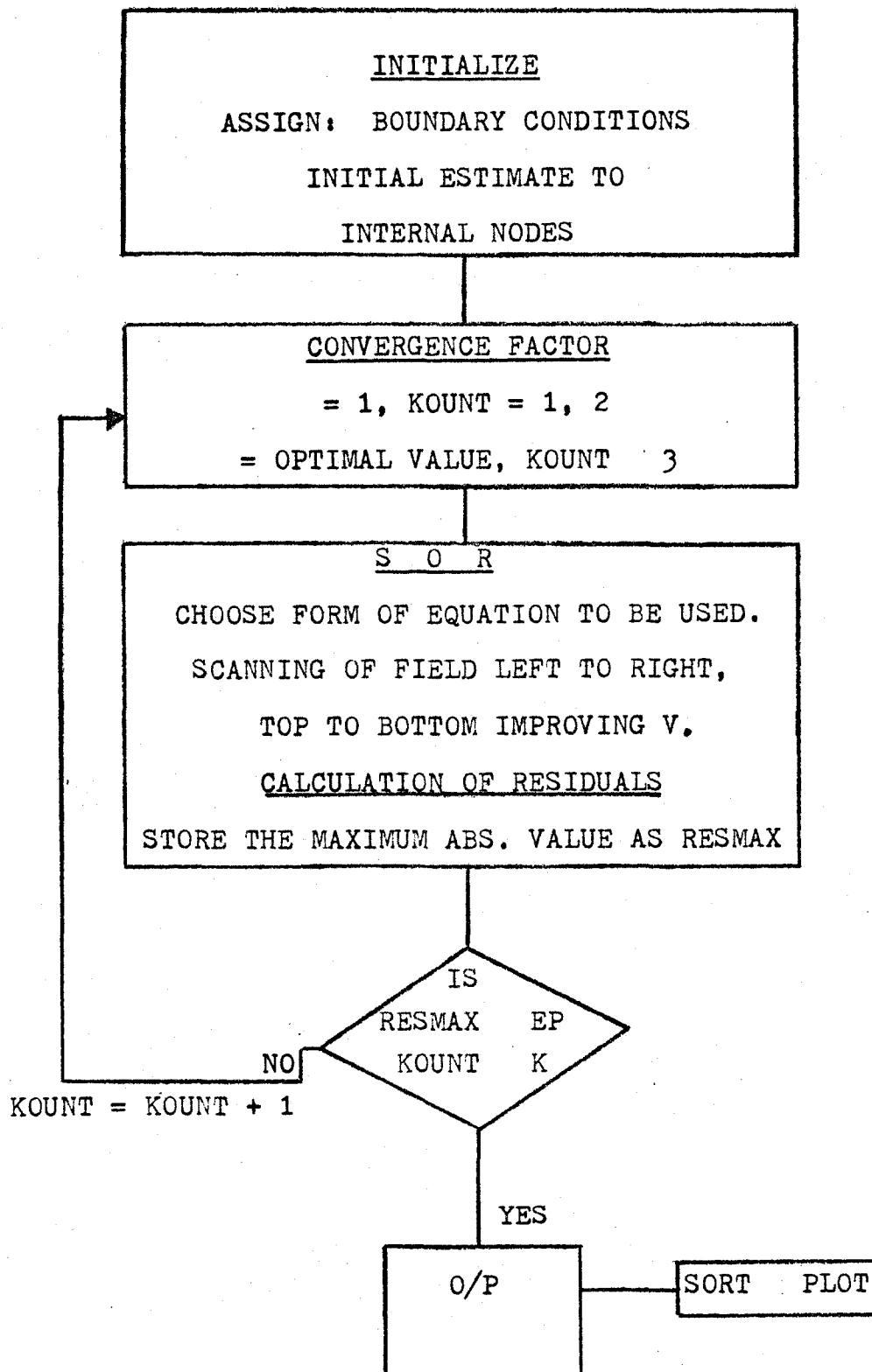


Fig. 3.2 SOR Computer Flow Chart

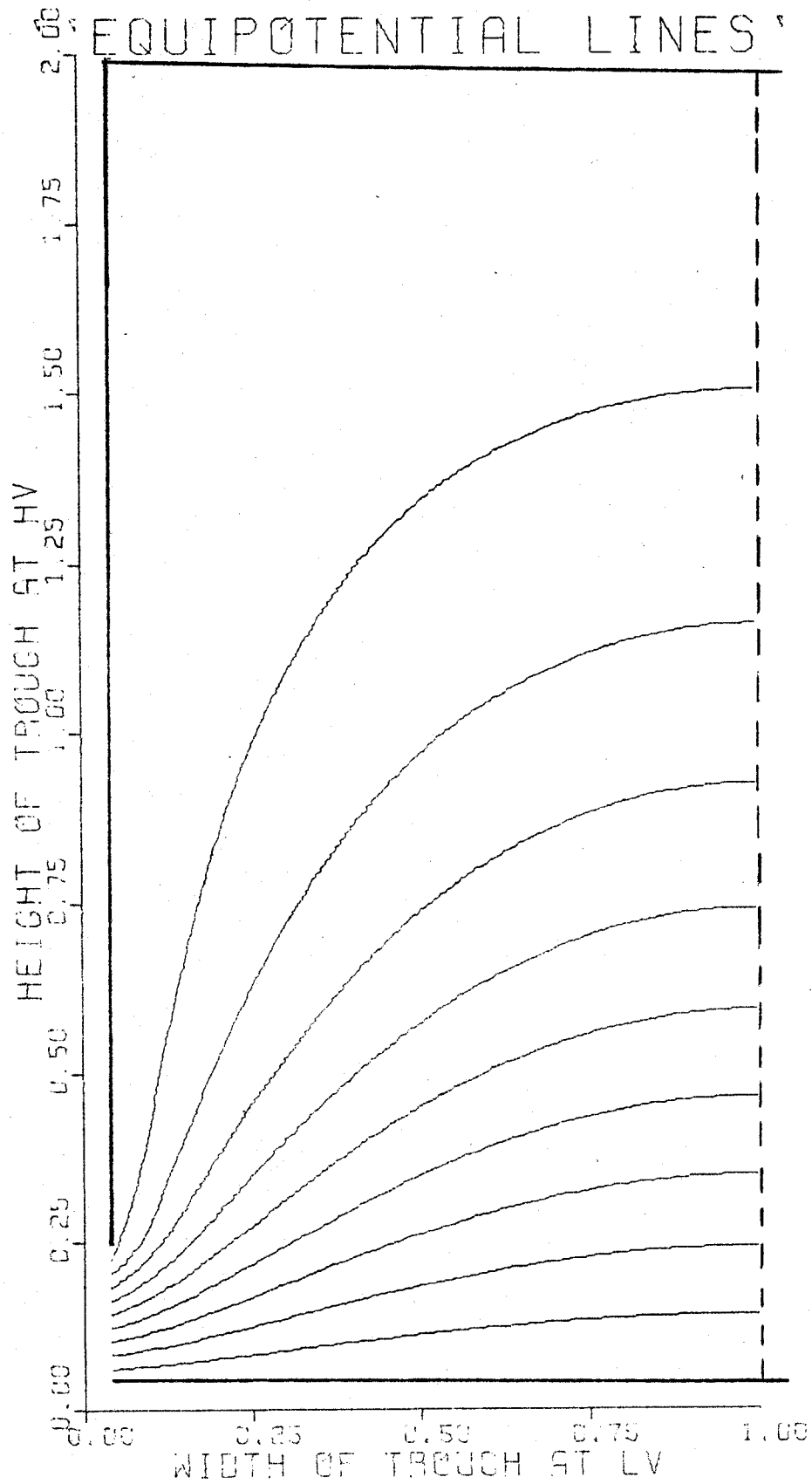


Fig. 3.3 Equipotential lines for a Rectangular Trough
(computer plot)

3.2.3. Application of the SOR Technique to the Field of an infinitely extending region

Formulation of the infinitely extending problem in finite difference simultaneous equations produces an infinitely large set of simultaneous equations. Methods have been developed for transforming the infinitely extending problem region into a finite one without appreciably disturbing the field in the region of interest. These methods introduce an artificial boundary either by physically altering the problem or by iteratively relaxing the artificial boundary simulated by charges on electrodes and the polarization charge on dielectric interfaces. Before describing either method two changes in equation (3.9) that are essential for both methods are given first.

To avoid division by zero when $r = 0$ at the axis of rotational symmetry, the second term in equation (3.3) is evaluated as a limit as $r \rightarrow 0$. Using L'Hopital's rule,²³

$$\lim_{r \rightarrow 0} \frac{1}{r} \frac{\partial V}{\partial r} = \frac{\partial^2 V}{\partial r^2} \quad \text{and remembering that } V_{i,j-1} = V_{i,j+1},$$

$W = Q$ for (i,j) on the axis of rotation symmetry equation (3.9) becomes

$$V_{i,j} = \left(\frac{V_{i+1,j}}{P(S+P)} + \frac{V_{i-1,j}}{S(S+P)} + \frac{2 V_{i,j+1}}{Q^2} \right) \frac{1}{1/SP + 2/Q^2} \quad (3.15)$$

For nodes on dielectric interfaces it is necessary to take into account the different dielectric constants.

For this purpose Laplace's equation (3.1) is developed from a closed curve integral of the gradient of a scalar function V with respect to the vector normal to the closed curve. The detailed development is not given here but the resulting form of equation (3.9) for node (r_j, z_i) on the dielectric interface is given.²⁴

$$V_{i,j} = \frac{1}{FKT} \left(V_{i+1,j} * FK1 + V_{i-1,j} * FK5 + V_{i,j+1} * FK3 + V_{i,j-1} * FK7 - V_{i,j} * FKT \right) \quad (3.16)$$

$$\text{where } FK1 = \left(1 + \frac{Q}{4R}\right)E1 + \left(1 - \frac{W}{4R}\right)E8$$

$$FK3 = \left(1 + \frac{P}{2R}\right)E2 + \left(1 + \frac{S}{2R}\right)E3$$

$$FK5 = \left(1 + \frac{Q}{4R}\right)E4 + \left(1 - \frac{W}{4R}\right)E5$$

$$FK7 = \left(1 - \frac{S}{2R}\right)E6 + \left(1 - \frac{P}{2R}\right)E7$$

$$FKT = FK1 + FK3 + FK5 + FK7$$

$E1, E2, \dots E8$ are the relative permittivities of the media in the eight half octants surrounding node (r_j, z_i) , the octants being numbered clockwise.

Returning to the two methods of introducing an artificial boundary, the first involves assigning $V = 0$ for nodes far from the region of interest or assigning a zero flux condition for such nodes. It is necessary to increase the grid size in the outer region to save on computer time and memory requirements. This method was applied on an insulator model. The zero flux condition

was used for nodes radially distant from the axis and $V = 0$ was assigned for these in the z direction. The grid size was doubled in the outer region. Different values of the convergence factor were used to try and obtain the optimum. However, the SOR technique gave unstable results even for unity convergence factor and the time requirements were uneconomically too high. Most of the time was used on responding to the many logical equations necessary for use of either equation (3.9), equation (3.15) or equation (3.16) and the associated different dielectric constants, avoiding application of SOR at electrode configurations.

The other method of boundary relaxation is relatively new in electrostatics. It involves setting up an artificial boundary enclosing the region of interest. The potential at this boundary is given by considering the effect of charges in the whole inner region, that is on electrodes, and polarization charge on dielectric interface. SOR is applied to the whole region to obtain improved values of V on all the inner nodes which in turn are used to evaluate the boundary values of V by charge simulation. This method has only been used for simple electrode and dielectric interface configurations.²⁵ In three dimensions these charges become ring charges each producing a potential represented by an elliptic integral. This method is more promising than the first; however, the finite element

method of section 3.3 was found to be superior in terms of time requirements and versatility. Furthermore, media-interfaces do not require any special consideration during computation.

3.3. The Finite Element Method

In the finite element method the solution to a complicated engineering field problem is approximated by subdividing the region of interest and representing the solution within each subdivision or element by a relatively simple function. Such a function is called a displacement function or simply an interpolation function; a polynomial is the common form of an interpolation function. The interpolation function within each element is substituted directly into the governing field equation (Laplace's equation, say) to obtain the nodal value equations. This is known as a direct approach of determining element properties. The elemental properties are then assembled to form simultaneous equations which are solved to obtain the nodal values of V .

The finite element method of obtaining a solution to any continuum problem thus follows an orderly step-by-step procedure:

1. Subdivision of the Continuum
2. Selection of the Interpolation Function
3. Determination of the Element Properties
4. Assembling the Element Properties to obtain the System Equations

5. Solving the System Equations
6. Additional Computations, if desired.

3.3.1. Statement of the Problem

In this work the finite element method is developed by solving Laplace's equation in a continuum composed of a truncated cone, or frustrum, with a partially conducting outer thickness on the sides and electrodes on the two ends; using the six-step procedure listed above. Laplace's equation in three dimensions with rotational symmetry can also be stated as

$$\frac{1}{r} \frac{\partial}{\partial r} \left(r \frac{\partial V}{\partial r} \right) + \frac{\partial^2 V}{\partial z^2} = 0 \quad (3.17)$$

In each element, the variation of r depends on the size of the element. Therefore in a small element the value of r can be taken to be constant and equal to the value at the centroid of the element, \bar{r} . In this way equation (3.17) becomes

$$\frac{\partial^2 V}{\partial r^2} + \frac{\partial^2 V}{\partial z^2} = 0 \quad (3.18)$$

in each element.²⁶

The problem is first solved in the partially-conducting region and using the values of V on the nodes of the inner surface the system for the dielectric region is solved.

3.3.2. Subdividing the Continuum

A variety of element shapes may be used to discretize the continuum into elements depending on the type of

problem.²⁷ The number and type of elements to be used in a given problem is a matter of engineering judgement. One has to rely on the experience of others for guide lines as no specific guidelines can be given for choosing the optimum element for a given problem because the type of element that yields good accuracy with short computing time is problem dependant.

For two-dimensional and three-dimensional axisymmetric problems requiring continuity only of the field variable V at element interfaces, the three node triangular element has been used by many analysts because of its simplicity and versatility. The frustrum was divided into such elements as shown in Fig. 3.4. In the finite element method media-interfaces are accounted for by simply dividing each region separately but allowing for continuity at the interface as shown in Fig. 3.4. All the nodes are then numbered systematically and depending on the complexity of the geometry of the continuum the nodes can be generated automatically on the computer.

3.3.3. Determination of the Interpolation Function

In determining the interpolation function to approximately represent the variation of the field variable V in each element, three conditions must be met for convergence to be rigorously assured (with increasing number of elements) in the finite element method.

- a) The interpolation function must be continuous within

'CONTINUUM SUBDIVIDED INTO ELEMENTS'

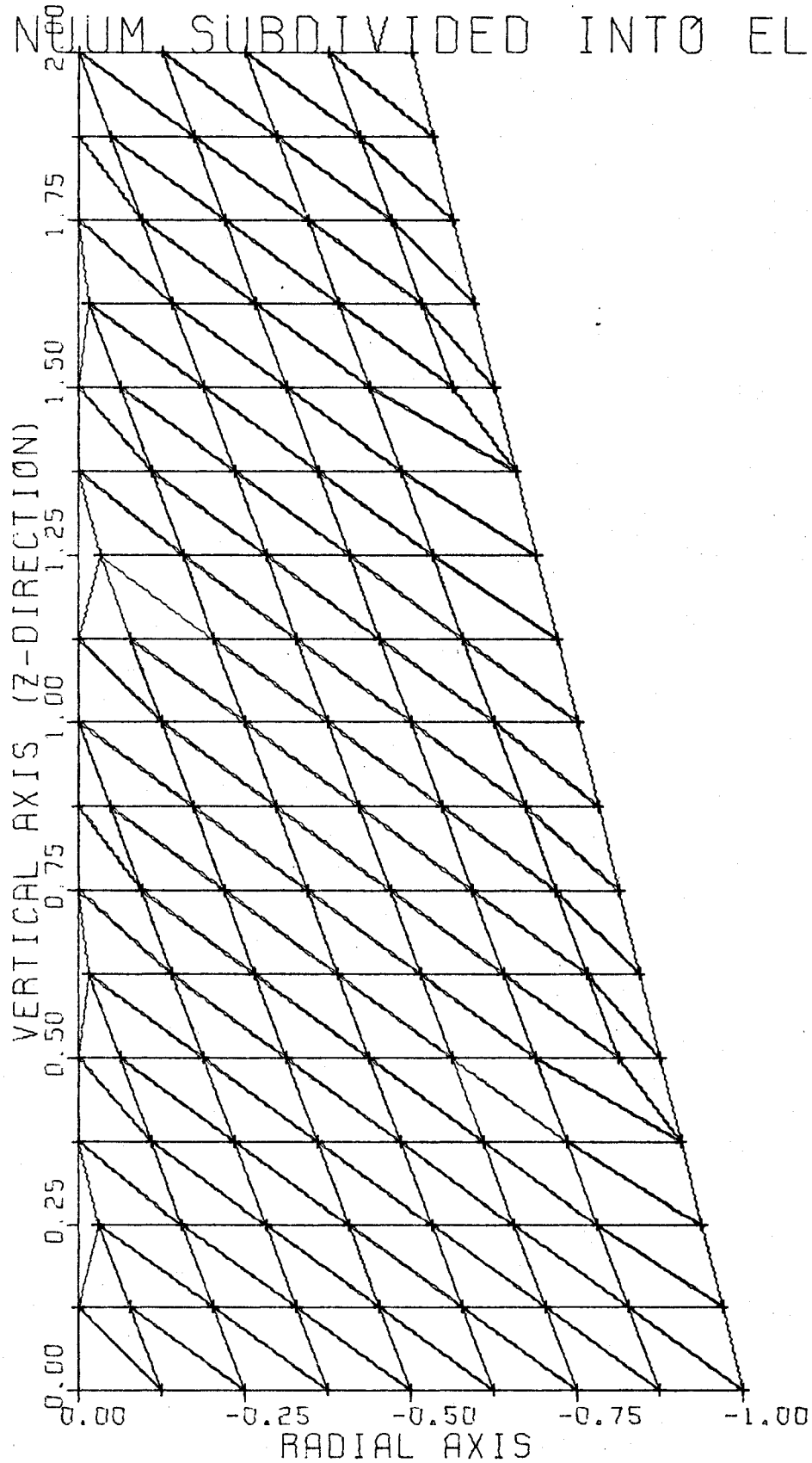


Fig. 3.4 Frustum Subdivided into Elements (computer plot)

the elements, V must be compatible or conforming between adjacent elements, and the value of V along the side of an element must depend only on its values at the nodes occurring on that side.

b) The derivative of the field variable, V in this case, must be constant for that element.

c) The interpolation function must allow for the constant electric stress of the element.

Furthermore, selection of the order of the interpolation function must be such that the pattern is independent of the orientation of the local coordinate system, that is to say it is geometrically invariant. Polynomials have been found to be suitable interpolation functions and equation (3.19) gives the general form of a polynomial that would satisfy the above requirements for two independent variables.²⁸

$$V(x,y) = a_1 + a_2x + a_3y + a_4x^2 + a_5xy + a_6y^2 + \dots + a_my^n$$

$$\sum_{i=1}^{n+1} i \quad (3.19)$$

where $m = \sum_{i=1}^{n+1} i$ is the number of terms corresponding to the

number of nodes of the element.

Consider element e in Fig. 3.4. The plane passing through nodal values of V associated with e can be described by the equation

$$v^{(e)}(x,y) = A^{(e)} + B^{(e)}x + C^{(e)}y \quad (3.20)$$

The constants $A^{(e)}$, $B^{(e)}$, and $C^{(e)}$ can be expressed in terms of the coordinates of the element's nodes and the nodal values of V by forming equation (3.20) at each node 1, 2, 3 numbered clockwise and then solving the three simultaneous equations for $A^{(e)}$, $B^{(e)}$ and $C^{(e)}$ (see Appendix B). On substituting for the three constants in (3.20) we get

$$v^{(e)}(x,y) = \left((a_1 + b_1x + c_1y)V_1 + (a_2 + b_2x + c_2y)V_2 + (a_3 + b_3x + c_3y)V_3 \right) / 2\Delta \quad (3.21)$$

where,

$$2\Delta = \begin{vmatrix} 1 & x_1 & y_1 \\ 1 & x_2 & y_2 \\ 1 & x_3 & y_3 \end{vmatrix}$$

= twice the area of triangle e

defined by vertices 1,2,3,

$$a_1 = x_2y_3 - x_3y_2, \quad b_1 = y_2 - y_3, \quad c_1 = x_3 - x_2 \text{ and}$$

the other coefficients are obtained by a cyclic permutation of the subscripts 1, 2, and 3.

In matrix form, equation (3.21) can be represented as

$$\begin{bmatrix} v^{(e)}(x,y) \end{bmatrix} = (N^{(e)}) \begin{bmatrix} v^{(e)} \end{bmatrix} \quad (3.22)$$

where $(N^{(e)}) = (N_1, N_2, N_3)$ and

$$N_i = \frac{a_i + b_ix + c_iy}{2\Delta} \text{ with } i = 1, 2, 3, \text{ is the interpolation function and } \begin{bmatrix} v^{(e)} \end{bmatrix} = \begin{bmatrix} v_1 \\ v_2 \\ v_3 \end{bmatrix}. \quad v_i, i = 1, 2, 3$$

are the nodal values of V .

If the continuum contains NE elements the complete representation of the field variable V is given by

$$\begin{aligned} V(x,y) &= \sum_{e=1}^{NE} v^{(e)}(x,y) \\ &= \sum_{e=1}^{NE} (N^{(e)}) \left[v^{(e)} \right] \end{aligned} \quad (3.23)$$

Equations (3.22) and (3.23) are of general validity irrespective of the form of the interpolation function and element shape.

3.3.4. Finding the Element Properties

To determine the field variation in each element according to the governing Laplace's equation, four approaches have been developed.²⁹ The direct approach given at the beginning of this section (3.3) is very simple and is limited to simple unidimensional fields. The most popular approach is the variational approach. An extremal principle is used with the finite element approximations to derive the element properties in terms of nodal values. Unless a functional can be obtained from the extremal principle for a given type of problem, the variational approach can not be applied. Another approach is the Energy balance approach. It requires no variational statement. The necessary elemental relations are obtained by considering local energy balances. Finally, the Method of Weighted Residuals (MWR) approach involves choosing an approximating function to the field variable and minimizing

the resulting residual or error on substitution into the governing field equation according to a certain criteria. This approach requires no functional and was found to be particularly suitable for this work. Its development follows here below.

Let the dependant field variable V be approximated by

$$\begin{aligned} V &\approx V^{(e)} \\ &= \sum_{i=1}^m N_i V_i \end{aligned} \quad (3.24)$$

N_i are the assumed functions and V_i are the unknown parameters. The m functions N_i are chosen to satisfy the global boundary conditions. On substitution of (3.24) into (3.1) a residual R results

$$\nabla^2 V^{(e)} = R \quad (3.25)$$

The MWR seeks to determine the m unknown(s) V_i 's in such a way that the residual R over the entire continuum vanishes in some average sense. A weighted average of the error is formed by weighting R with weighting functions W_i ($i=1$ to m) and specifying that if this average vanishes over the entire solution domain, D , then the value of R will tend to zero.

$$\begin{aligned} \int_D \nabla^2 V^{(e)} W_i dD &= \int_D R W_i dD \\ &= 0 \quad i = 1, 2, \dots, m \end{aligned} \quad (3.26)$$

Once the weighting functions are specified then equations (3.26) form a set of ordinary differential

equations to be solved for the m values of V, V_i . It can be shown that as m tends to very large values, $v^{(e)}$ tends to the exact solution V . A broad choice of weighting functions or error distribution principles exist. Galerkin's method is the error distribution principle most often used when MWR is used with the finite element method. In Galerkin's method the weighting functions are chosen to be the same as the approximating functions (interpolation functions in this case) used to represent V in equation (3.24). Thus $W_i = N_i, i = 1, 2, \dots, m$. For each element $D^{(e)}$ which make up domain D equation (3.26) becomes

$$\int_{D^{(e)}} \nabla^2 v^{(e)} N_i d D^{(e)} = 0 \quad (3.27)$$

Integration by parts is used to introduce the influence of the natural boundary conditions in (3.27) for all elements at such boundaries since the N_i s were not chosen so as to satisfy any boundary conditions (see section 3.3.3). Writing (3.27) in two dimensional coordinates gives

$$\int N_i \frac{\partial^2 v^{(e)}}{\partial x^2} dx dy + \int N_i \frac{\partial^2 v^{(e)}}{\partial y^2} dx dy \quad (3.28)$$

Integration by parts of the first term in (3.28) gives

$$\begin{aligned} \int N_i \frac{\partial^2 v^{(e)}}{\partial x^2} dx dy &= \int_{l^{(e)}} N_i \frac{\partial v^{(e)}}{\partial x} dy \\ - \int \frac{\partial v^{(e)}}{\partial x} \frac{\partial N_i}{\partial x} dx dy &= \int_{l^{(e)}} N_i \frac{\partial v^{(e)}}{\partial x} n_x dl - \\ \int \frac{\partial v^{(e)}}{\partial x} \frac{\partial N_i}{\partial x} dx dy & \end{aligned} \quad (3.29)$$

where n_x is the x -component of the unit normal to the boundary and dl is the differential arc length along the boundary. Treating the second term of (3.28) similarly, on substitution (3.28) becomes

$$\int_{D(e)} \frac{\partial V(e)}{\partial x} \frac{\partial N_i}{\partial x} + \frac{\partial V(e)}{\partial y} \frac{\partial N_i}{\partial y} dx dy - \int_{D(e)} N_i dx dy - \int_{l(e)} N_i \left(\frac{\partial V(e)}{\partial x} n_x + \frac{\partial V(e)}{\partial y} n_y \right) dl = 0 \quad (3.30)$$

The normal derivative of V is zero at the sides of the partially-conducting region of the frustrum of Fig. 3.4 and at the line of rotational symmetry. Thus the line integral in (3.30) is identically zero. The values of $V(e)$ (x, y) and N_i as given in (3.22) are substituted into (3.30) giving

$$\frac{b_i (b_1 \quad b_2 \quad b_3) [V(e)]}{4 \Delta} + \frac{c_i (c_1 \quad c_2 \quad c_3) [V(e)]}{4 \Delta} \int dx dy = 0 \quad (3.31)$$

$i = 1, 2, 3$

The integral in (3.31) is the elemental area Δ (see Appendix B). In matrix form equations (3.31) are given by

$$[S(e)] [V(e)] = [R(e)] \quad (3.32)$$

$S(e)$ is a square matrix the typical element of which is

$$S_{ij} = \frac{b_i b_j + c_i c_j}{4 \Delta} \quad \begin{matrix} i = 1, 2, 3 \\ j = 1, 2, 3 \end{matrix}$$

$$\text{and } R(e) = \begin{bmatrix} 0 \\ 0 \\ 0 \end{bmatrix}$$

Equation (3.32) gives the elemental properties. Using the approximation of (3.18) it is only necessary to multiply S_{ij} by $2\pi r$ to give the three-dimensional axisymmetric form of equation (3.32).

3.3.5 Assembling the Element Properties

Equations of the form (3.32) obtained for each element are assembled to form matrix equations expressing the behaviour of the entire continuum. The basis for the assembly procedure stems from the conformity requirement of V , that is at a node where elements are interconnected, V has the same value for each element sharing that node.

When all nodes have the same coordinate system the assembly procedure follows a systematic execution of equation (3.33) for all elements, suitable for a digital computer. Such a computer program is given in Appendix C.

$$\sum_{e=1}^{NE} \sum_{i=1}^{NN} [S^{(e)}] [V^{(e)}] = [R^{(e)}] \quad (3.33)$$

The inner summation is taken for all the nodes NN and the latter for all the elements resulting in $[S] [V] = [R]$. The resulting assembled matrix is sparsely populated and has the non-zero terms clustered about the main diagonal (banded) reflecting the connectivity of the finite element mesh. Numbering the nodes causes the system matrices to be banded, depending on the nodal numbering scheme the band width can be minimized.

The system equations are then modified to account for the boundary conditions of the problem, that is, specified values of V , otherwise they form a singular matrix. This is done by modifying the matrices $[S]$ and $[R]$ in equation (3.33) as follows. If at node i , V_i is specified then i^{th} row and i^{th} column of $[S]$ are set equal to zero and S_{ii} is set equal to unity. The term R_i in $[R]$ is replaced by the known value of V_i . Each of the remaining terms of $[R]$ is modified by subtracting from it the product of V_i and the appropriate column term from the original $[S]$ matrix. Consider a simple illustrative case where

$$[S] = \begin{bmatrix} S_{11} & S_{12} & S_{13} & S_{14} \\ S_{21} & S_{22} & S_{23} & S_{24} \\ S_{31} & S_{32} & S_{33} & S_{34} \\ S_{41} & S_{42} & S_{43} & S_{44} \end{bmatrix} \quad \text{and} \quad [R] = \begin{bmatrix} R_1 \\ R_2 \\ R_3 \\ R_4 \end{bmatrix}$$

with V_1 and V_3 specified as boundary values of V at nodes 1 and 3. Accounting for the boundary condition results in

$$\begin{bmatrix} 1 & 0 & 0 & 0 \\ 0 & S_{22} & 0 & S_{24} \\ 0 & 0 & 1 & 0 \\ 0 & S_{42} & 0 & S_{44} \end{bmatrix} \begin{bmatrix} V_1 \\ V_2 \\ V_3 \\ V_4 \end{bmatrix} = \begin{bmatrix} V_1 \\ R_2 - S_{21}V_1 - S_{23}V_3 \\ V_3 \\ R_4 - S_{41}V_1 - S_{43}V_3 \end{bmatrix}$$

as the modified matrix equations of the system ready for solving.

3.3.6 Solving of the System Equations

Direct or Iterative schemes (e.g. Gaussian elimination or Gauss-Seidel methods respectively) are the basic methods used to solve the system equation for the field variable V .

However, methods that take advantage of the symmetry, sparseness and bandedness properties that usually characterize $[S]$ are far more convenient in this case. A subroutine available in the computer library (SIMQ) was used and the results were used to plot equipotential lines given in Fig. 3.5. Subroutine CONTUA given in Appendix C was written for this purpose.

3.3.7 Additional Computations

The electric field stress was calculated for each element by Subroutine FIELD (Appendix C) using the calculated values of V at each node. Equation (3.23) gives the variation of V within the element in terms of the nodal values of V i.e.

$$V^{(e)}(x,y) = N_1V_1 + N_2V_2 + N_3V_3$$

taking the gradient with respect to x and then y gives the corresponding field stress components E_x and E_y

$$\begin{aligned} E_x &= \frac{\text{grad } V^{(e)}(x,y)}{x} \\ E_y &= \frac{\text{grad } V^{(e)}(x,y)}{y} \end{aligned} \quad (3.34)$$

the resultant of which is

$$E^{(e)} = \sqrt{E_x^2 + E_y^2}$$

Fig. 3.6 gives the electric field stress in each element. This stress can be thought of as acting at the centroid of the element.

The finite element method as developed here was applied to a power line insulator and the results are

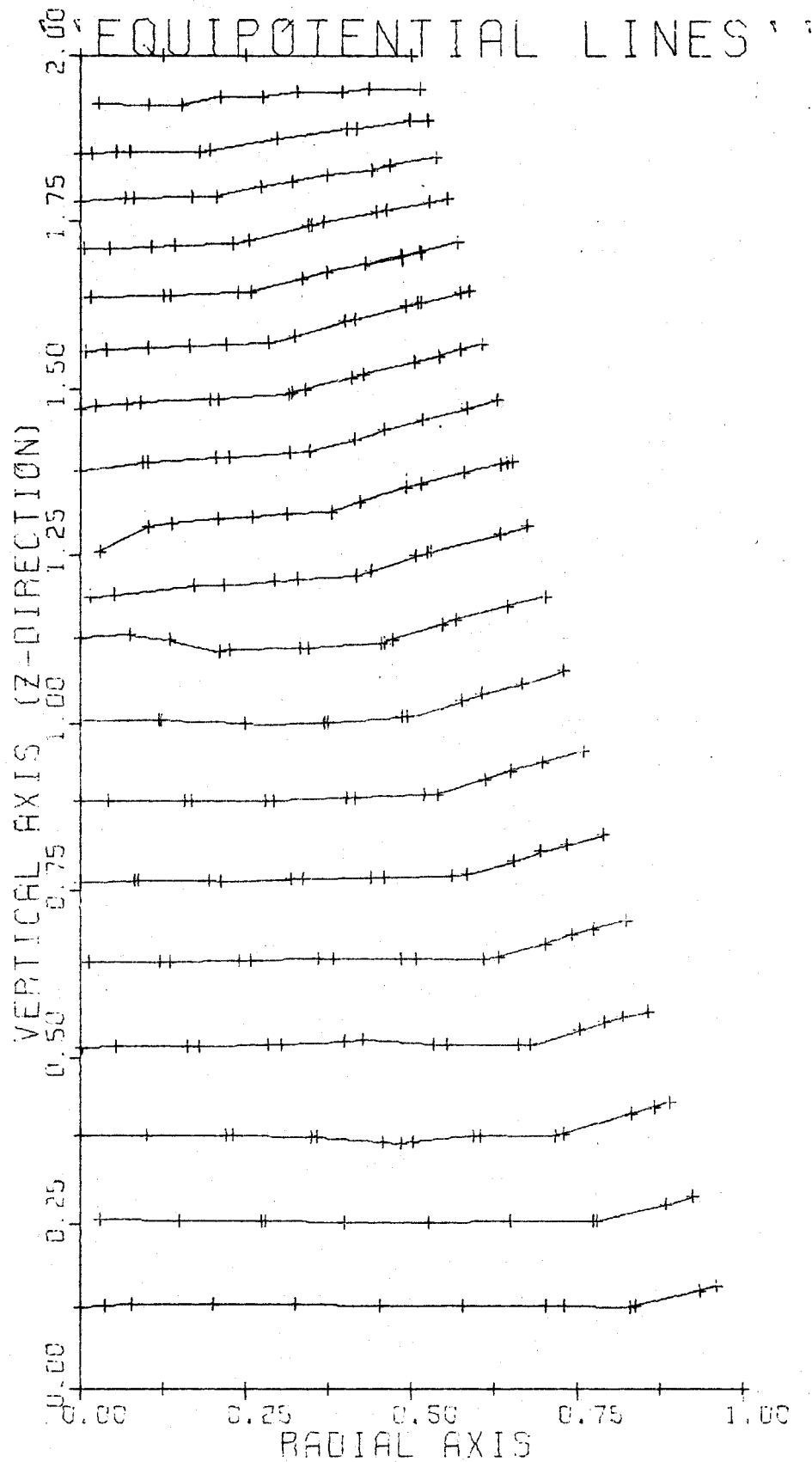


Fig. 3.5 Equipotential Lines for the Frustrum

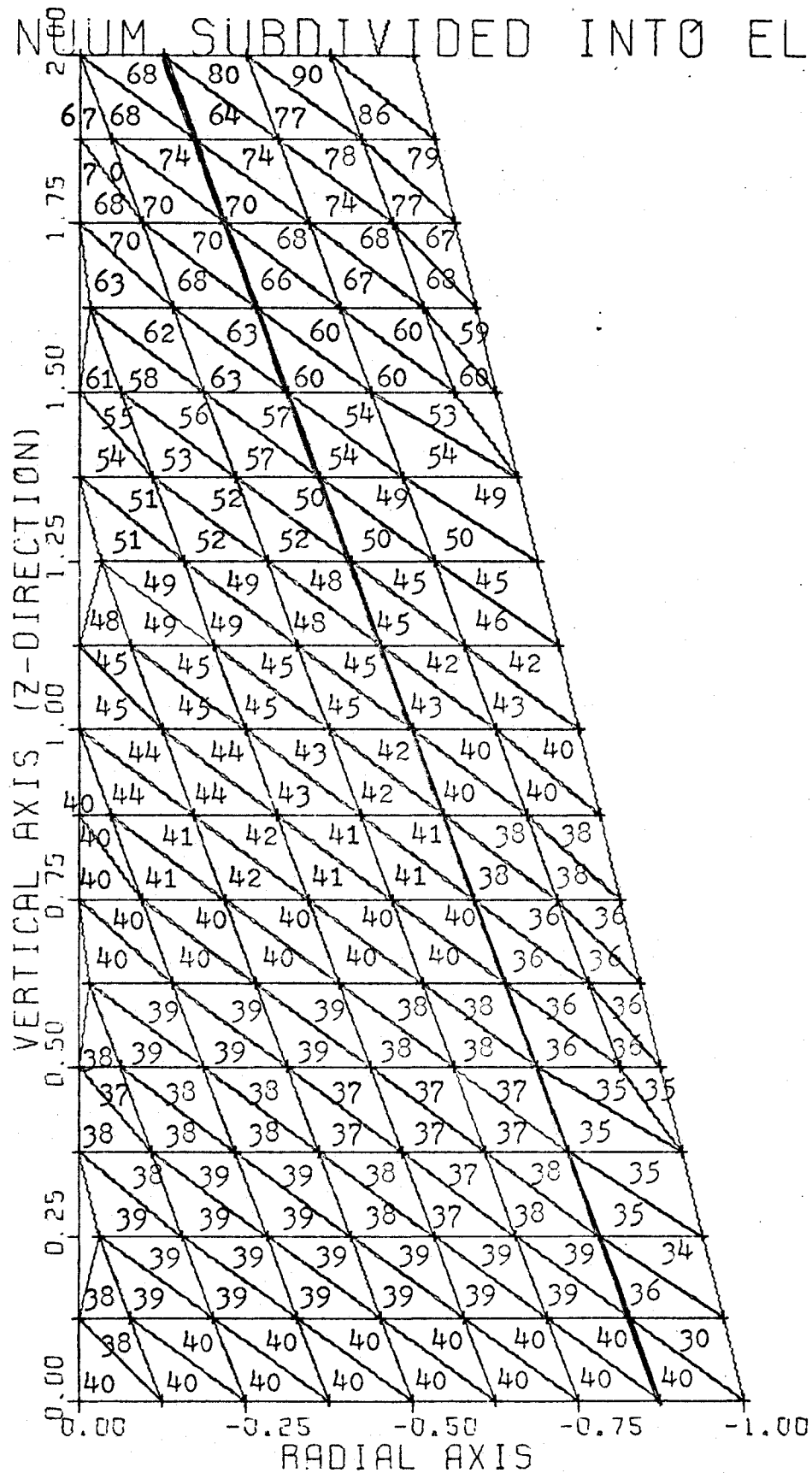


Fig. 3.6 Elemental Stress in the Frustrum

given in the next chapter.

CHAPTER IV

DESIGN OF AN ANTI-POLLUTION INSULATOR

About four years ago, research work started here at the University of Windsor to develop a partially conducting material to be used in power line insulators for contaminated environment. Such material was required to have a positive temperature coefficient (to avoid thermal instabilities associated with current semi-conducting glazes), very high resistance to tracking to avoid surface deterioration due to discharges, and high dielectric strength. Silicone carbide filled with Adeprene was developed and a great deal of research work has been devoted to determining the appropriate material proportions to give the required conductivity, current-voltage characteristics and other properties.³⁰

A non-conventional power line insulator design concept is to be used in which the insulator body is made up of three regions; an inner core, a middle region and partially-conducting outer thickness. Fibre glass forms the inner core to provide the required mechanical strength to withstand the various loading conditions. Epoxy forms the middle region and provides the required dielectric strength, and silicone carbide filled adeprene forms the partially-conducting outer thickness. Using a controllable outer thickness of the partially conducting material enables the designer to try and achieve uniform resistance-grading on the insulator surface (see section 4.2).

Our design concept could have been applied to existing geometries, however, it was decided that a geometry obtained by considering the effect of insulator shape on performance of insulators in contaminated areas would be a much better solution (together with uniform voltage distribution on the insulator surface) to the pollution problem.

4.1 Design Factors

For the design of an anti-pollution insulator, the following factors should be considered:

- a) Adequate leakage path length
- b) Geometry considerations
- c) Corona requirements
- d) Ample mechanical strength
- e) High ratio of impulse to normal flashover voltage
- f) Economic feasibility and Technological Considerations

All these factors with exception of b) have been used in conventional anti-fog insulator designs, however, in this work some of these factors have been modified in the light of the available information from both in-service tests and operational experience. Factors c) to f) are basic requirements for the successful and economic operation of any power line insulator irrespective of the type of environment. A review of all these factors follows.

- a) Adequate leakage path length

Any power line insulator should be designed with

adequate leakage path length per unit kilovolt of operating voltage so that flashover will always occur in the air path surrounding the insulator. Based on in-service tests and on operational experience it has been specified that, for slightly polluted areas, insulators should have a leakage path length of at least 2.5 cm per kV of operating voltage. Furthermore a good anti-fog insulator design should have a figure of merit, that is ratio of leakage path length to insulator height, of at least three.³¹

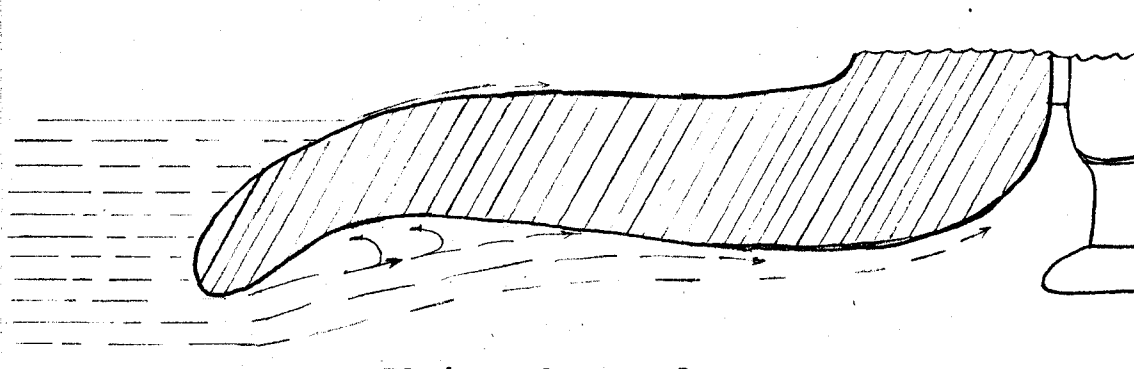
The necessity for adequate leakage path length is more emphasized by the fact that the risk of flashover depends on the leakage current which in turn depends on the surface resistance of the contaminated insulator and therefore the leakage path length. The leakage current phenomenon has already been covered in Chapter 2; it is sufficient here to only say that the limiting value of the leakage current (the maximum value before flashover) flowing on the surface of a polluted insulator has been found to be 1 mA. This value increases with diameter of the insulator.

b) Geometry considerations

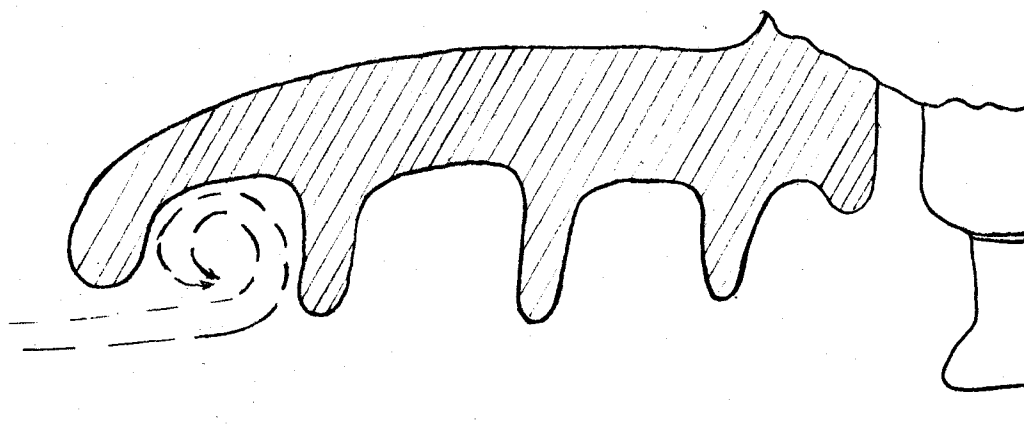
Provision of the specified leakage path does not in itself ensure good performance of the insulator in a polluted environment. In addition to being adequate, the leakage path length should be formed by a uniform and symmetrical geometry in order that the variations (of the surface resistance of different units, or different

parts of the same unit) shall be reduced as much as possible; otherwise the leakage path length per unit of system voltage becomes a criterion of limited application. The leakage path length (or the insulator surface) should be apportioned so as to strike a balance between the amount of insulator surface exposed to cleaning by wind and rain and the amount of sheltered surface. An anti-pollution insulator requires a suitable shed design to take advantage of the natural cleansing action of wind and rain. However, great care is required because both wind and rain are possible causes of trouble. Rain should strike the insulator surface with sufficient force to dislodge contamination particles so as not to rely only on the eddy action of wind and the splashing of rain for cleaning the hidden surfaces.

Insulators with a plain undersurface show remarkable reduction in the amount of dirt collected. This is due to the practically eddy-free air flow as shown in Fig. 4.1. A plain rod has the greatest possible length of naturally washed surface but to obtain adequate wet flashover characteristics sheds must be introduced on the rod. A single shed of small diameter will result in improved flashover voltage on the plain rod but at the loss of a certain amount of naturally washed surface. In Fig. 4.2, the wet flashover voltage is mainly determined by dimension x . The maximum value of x considering a 45° rainfall is obtained by increasing the diameter of the shed for a



Plain under surface;
little eddy formation



Ribbed under surface;
considerable eddy formation

Fig. 4.1 Flow of Air Past Insulator Under Surface

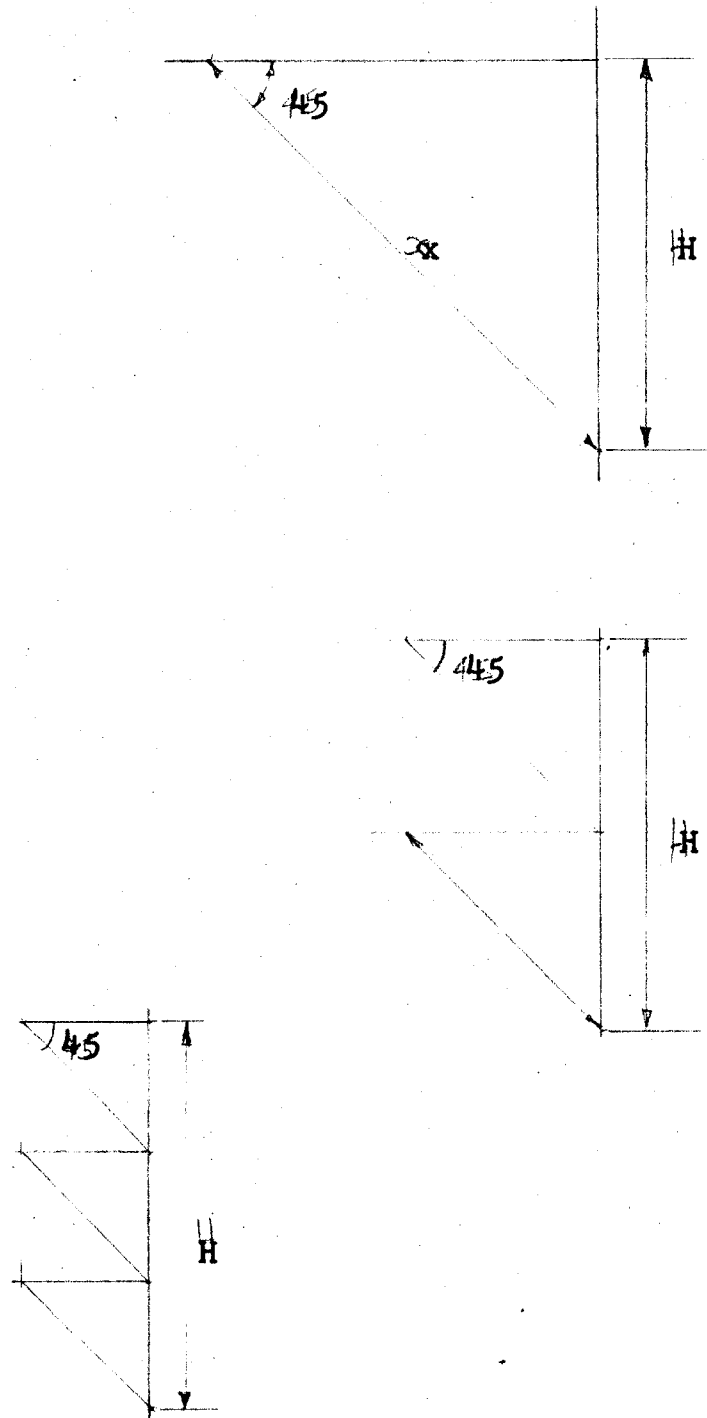


Fig. 4.2 Extent of Naturally-cleansed Surfaces
as affected by Number and Shape of Sheds

given height of the rod. The wet flashover characteristics so obtained can be achieved more economically (using less insulator material) by the use of a two - or even much more economically a three - shed design. To increase the number of sheds would increase the "shaded" vertical surface that would increase the surface area for air-born deposit. Needless to say that the more drooping these sheds are the greater will be the shaded regions.

Insulator geometry should, therefore, be designed to achieve the greatest possible length of cylindrical surface unbroken by sheds. At the same time the geometry should be designed to allow for at least half the leakage path length to remain dry under extreme conditions of rainfall and wind. Thus a compromise between these two requirements give the best design of insulator geometry.³² Research work done in Europe shows that, although shed inclination to the insulator stem is necessary, the deviation from the shed being perpendicular to the stem should be a "teen-angle".³³ A small inclination of the underside of the shade is necessary to stop dripping pollution-laden water from completely bridging the two electrodes. Furthermore sheds on a given insulator unit should not be of equal protrusion or diameter so as to avoid bridging between sheds that would otherwise occur during rainfall thus drastically reducing the amount of insulating surface. Conventionally for anti-fog designs the ratio of shed protrusion to

separation between sheds (of equal diameter) is required to be about 0.85 for insulators in a polluted environment.³⁴ The disadvantage here is that of the risk of rain bridging the sheds.

In this subsection non-conventional techniques for designing the insulator geometry have been introduced, the few conventional ones being greatly modified or completely rejected in the light of current information about the performance of anti-fog insulators in a polluted environment.

c) Corona requirements

Any power line insulator is required to be free from visible discharge up to a certain voltage, the corona voltage, which is usually fixed at twenty to forty per cent above the phase voltage. The object of this is to ensure as much as possible that the insulator is free from discharges which would give rise to excessive radio- and television-signal interference in the immediate vicinity. These discharges would also result in energy losses.

A uniform voltage distribution on the insulator would result in all portions of the air at the insulator surface being evenly stressed thus eliminating highly stressed local areas that would result in the breakdown of the surrounding air. The insulator surface should be smooth and proper contact between the insulator material and the electrodes and hardware at high voltage must be maintained for the corona onset voltage to be high.

d) Ample mechanical strength

Any power line insulator must be mechanically sound to support the line with adequate factor of safety under the most adverse conditions and to meet other requirements given in Chapter I. The mechanical loading on the insulator is mainly the weight of the conductor; however, adverse conditions of snow and heavy storms increase this loading. Lightning discharges and other high frequency arcs subject the insulator to excessive electromechanical stresses.

Insulators are rated either on the nominal working load multiplied by a factor of safety of three and half, or the minimum failing load. Electromechanical breaking strength (obtained by applying both a mechanical load and a voltage until the insulator fails either mechanically or electrically) is nowadays used to assess the performance of an insulator.³⁵

e) High ratio of impulse to normal frequency flashover

Insulators are designed to have an impulse ratio of at least 3.75. Higher values are necessary in the case of an anti-pollution insulator (see section 1.1). Impulse ratio is a design factor to ensure that insulators will flashover under a lightning arc and other high frequency surges rather than puncture.

f) Economic feasibility and technological considerations

From the preceding requirements it is evident that any insulator must be designed in the form such that it

will meet widely divergent conditions. From the manufacturing standpoint it is uneconomical to manufacture units of different mechanical strengths for different weights of conductors and climatic loadings and conditions. The most successful design is such that the same unit will operate satisfactorily under the most adverse conditions of loading and pollution with adequate factors of safety and at the same time will be economical enough for use on the less important lines.

Technological considerations limit the designer when attempting to achieve a compromise between the different requirements.

4.2 The Present Design

Before undertaking the design and construction (by casting) of the insulator, geometries of conventional post insulators were reviewed. Table 4.1 gives some of the characteristics of these insulators for preferred or standard system voltages. In particular, the 33 kV unit shown in Fig. 4.3 was considered. Taking half the length of this insulator the outer profile was designed according to the geometry requirements and in consideration of the other design criteria of the value system discussed in section 4.1. Having thus designed the profile and using 2 kV of operating voltage per inch of leakage path length the rating of the insulator was tentatively fixed for 46 kV system operation. The outer profile is shown in Fig. 4.4.

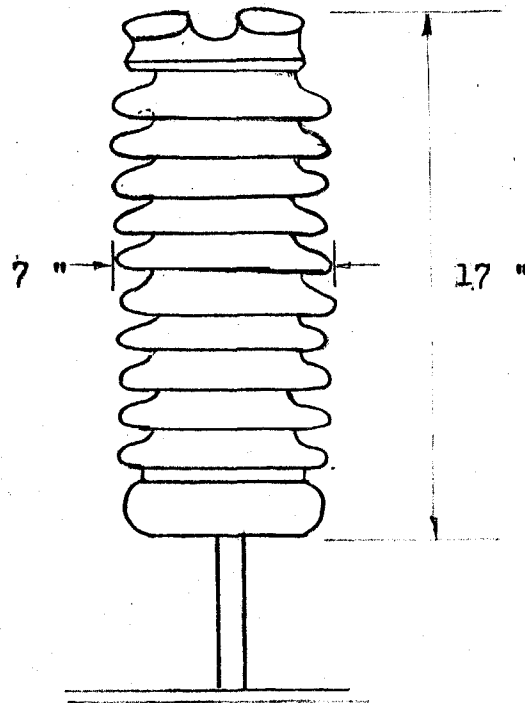
Nominal Preferred System Voltage	Wet F.O.V. kV	Impulse Withstand kV	Insulator Height (Post) mm	Max. Diam. of Insulating Part**mm	Min. Leakage Path Length mm
120V					
480V					
4.16kV					
4.8kV					
13.8	27	75	190	76	120
23	35	125	215	76	190
34.5	75	170	445	76	580
46	105	250	560	76	835
69	185	380	1020	127	1600
115	275	650	1500	127 (225)	2300
138	395	900	2100	127 (225)	3400
230	630	1425	3150	127 (225)	5600
345	740	1675	3850	127 (225)	6700
500 (550)	1600*				
700 (765)	2050*				

* Have been worked out using empirical formular

** Can be increased in cases of severe pollution

In each case mechanical strength can be 2, 4, 6, 8, 10 kN depending on load.

TABLE 4.1 (Produced from IEC, 273 of 1968)



leakage path length - 40 inches

dry arc distance - $14\frac{1}{2}$ inches

Fig. 4.3 33 kV Post Insulator

The concept of a controllable partially-conducting outer thickness can be used to attain uniform voltage distribution on the insulator surface and the required thermal distribution. The conductivity of the partially-conducting material governs the amount of heating (as opposed to leakage) current flowing in this material. The profile and thickness of this material governs the current distributions. The current flow in turn governs the voltage distribution on the insulator and the required thermal dissipation to avoid moisture condensation on the insulator surface. Designing for a uniform thermal dissipation on the insulator surface requires taking into consideration the extremely variable ambient temperature, radiational and convectional losses at the different parts of the insulator surface. Moreover, for two adjacent sheds, the heat lost at the surface of the lower shed will increase the ambient temperature around the underside of the upper shed. Therefore it is difficult to have uniform ambient thermal conditions around the entire insulator unit, making it extremely difficult to design for uniform thermal dissipation on the insulator surface. Therefore the uniform voltage distribution criteria was used to determine the thickness of the partially -conducting material.

The profile of Fig. 4.4 was subdivided into sub-regions depending on the geometric nature i.e. discs, segments and arcs. In three dimensions each of these sub-regions is a solid of revolution. For a given homogeneous

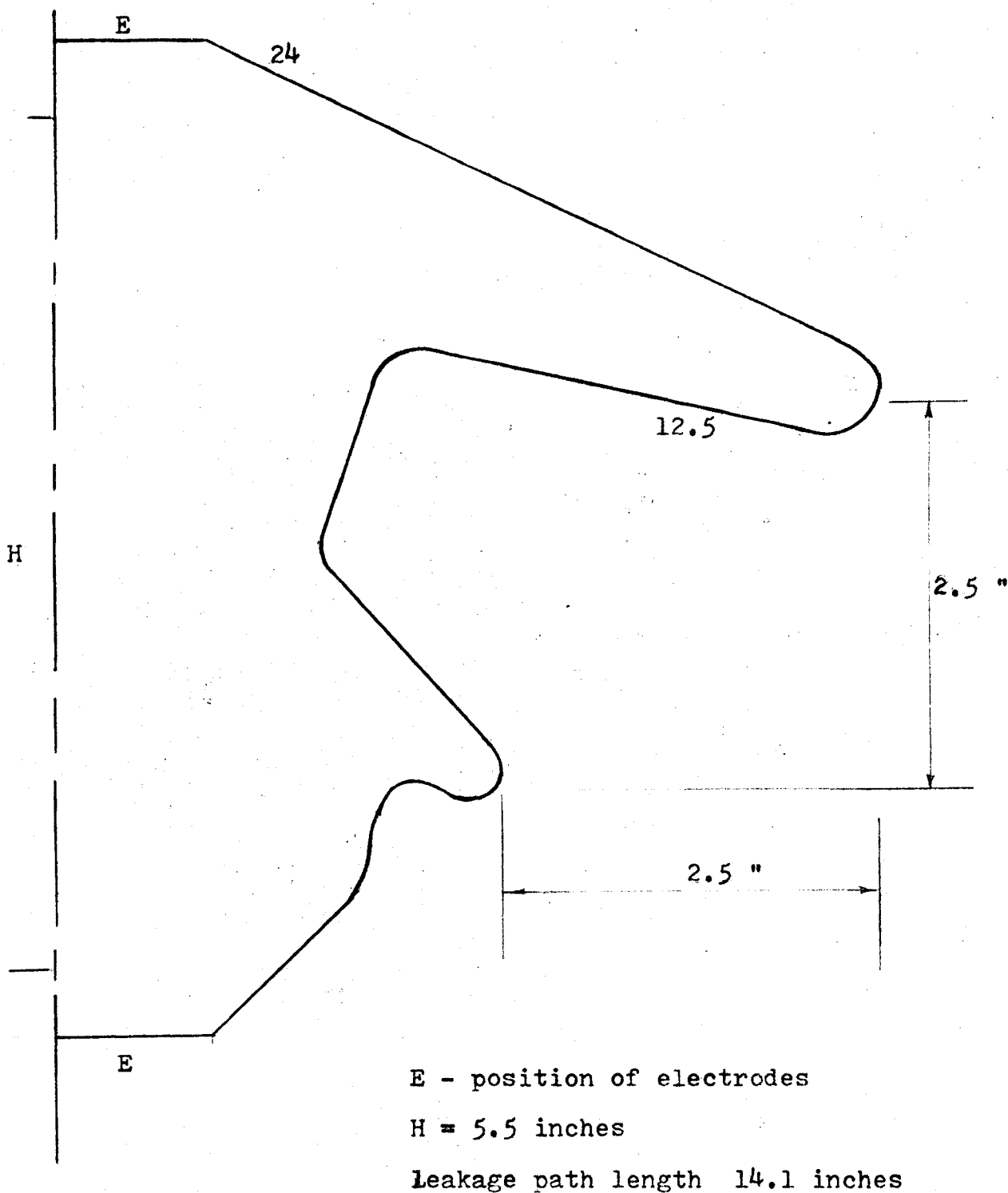


Fig. 4.4 Geometry of the Insulator Design

material the resistance to current flow in each subregion will vary directly as to length and inversely as to cross-section area of the path. The resistance will be directly proportional to length resulting in a uniform voltage distribution on the insulator surface, if the cross-section area is held constant for all the subregions. In two dimensions, the cross-section area would be the area obtained by considering a line perpendicular to the line forming the boundary of flow, in this case we consider the cross-section area of a solid of revolution. A value of the cross-section area that gave practical values of the thickness was chosen. For each of 25 subregions a value of the thickness t , was worked out and these points were joined with straight lines; thus achieving subregional uniform variation of potential but not necessarily uniform in each subregion. To achieve a completely uniform variation of potential the insulator would have to be subdivided into many more subregions to attain many more points for the inner curve. However, such effort would be futile as considerations for ease of manufacture would result in changes in the form of the inner profile. The resulting profile of the partially-conducting region is as shown in Fig. 4.6.

Originally the electrodes were to be prototype just to facilitate testing in the laboratory however ensuring complete contact with the different materials. The electrode shape was however, modified to avoid increasing the

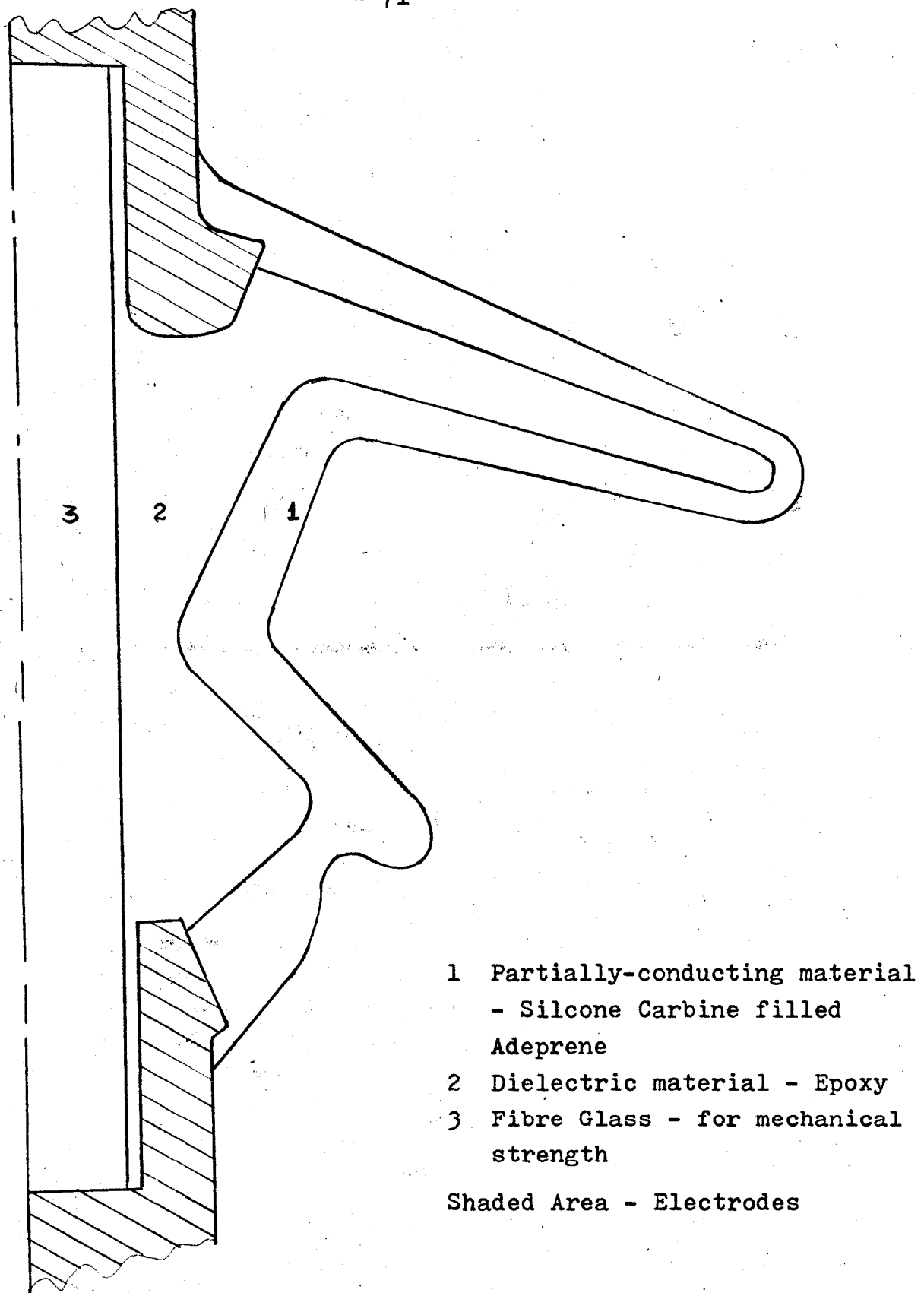


Fig. 4.5 The Insulator Design

leakage path length per kV than was necessary and other technological requirements.

The mold for casting the insulator is made of epoxy and is made up from three parts. The volume of the partially-conducting part is approximately 100 cu. in. and that of the dielectric material is approximately 60 cu. in.

4.3 Analysis of the electric field of the insulator design

The finite element method developed in Chapter III for a frustrum with a partially-conducting outer thickness was applied to the insulator design shown in Fig. 4.5. Due to the complexity of the insulator geometry, the elements could not be automatically generated. Fig. 4.6 shows the element pattern. Media interfaces are represented by element sides.

In calculating the field the two regions are considered separately. First, the partially-conducting region is solved by considering as a completely bounded problem, the natural boundary conditions are approximately those of a conductor (the normal derivative of potential is zero along the sides). The values of potential at nodes on the partially-conducting and dielectric media interface, so obtained, are used as specified boundary values in solving the dielectric region. Plots of equipotential lines were obtained for both regions using subroutine CONTUA. Fig. 4.7 shows the equipotential lines for the whole insulator in

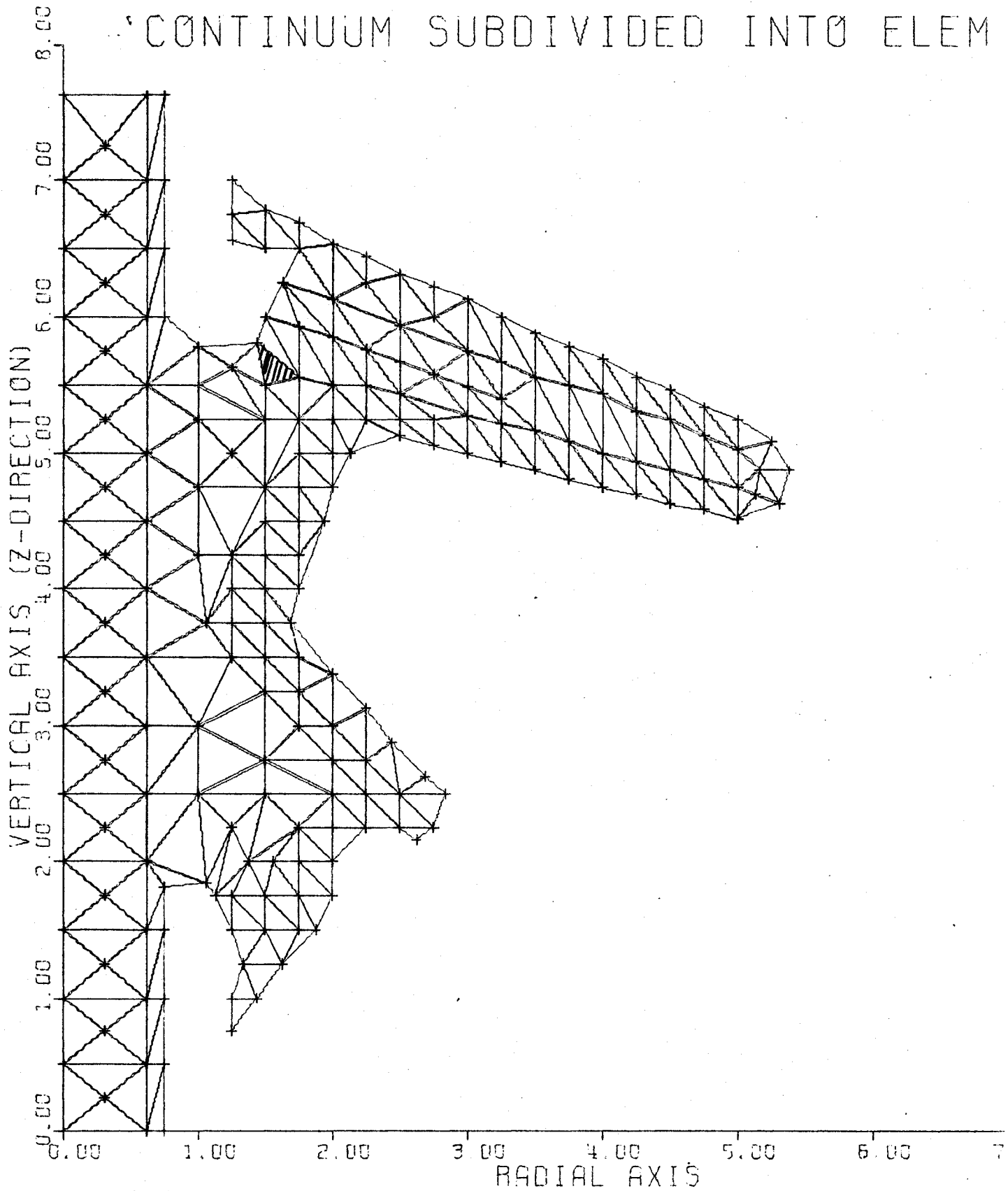


Fig. 4.6 Insulator Divided into Elements (computer plot)

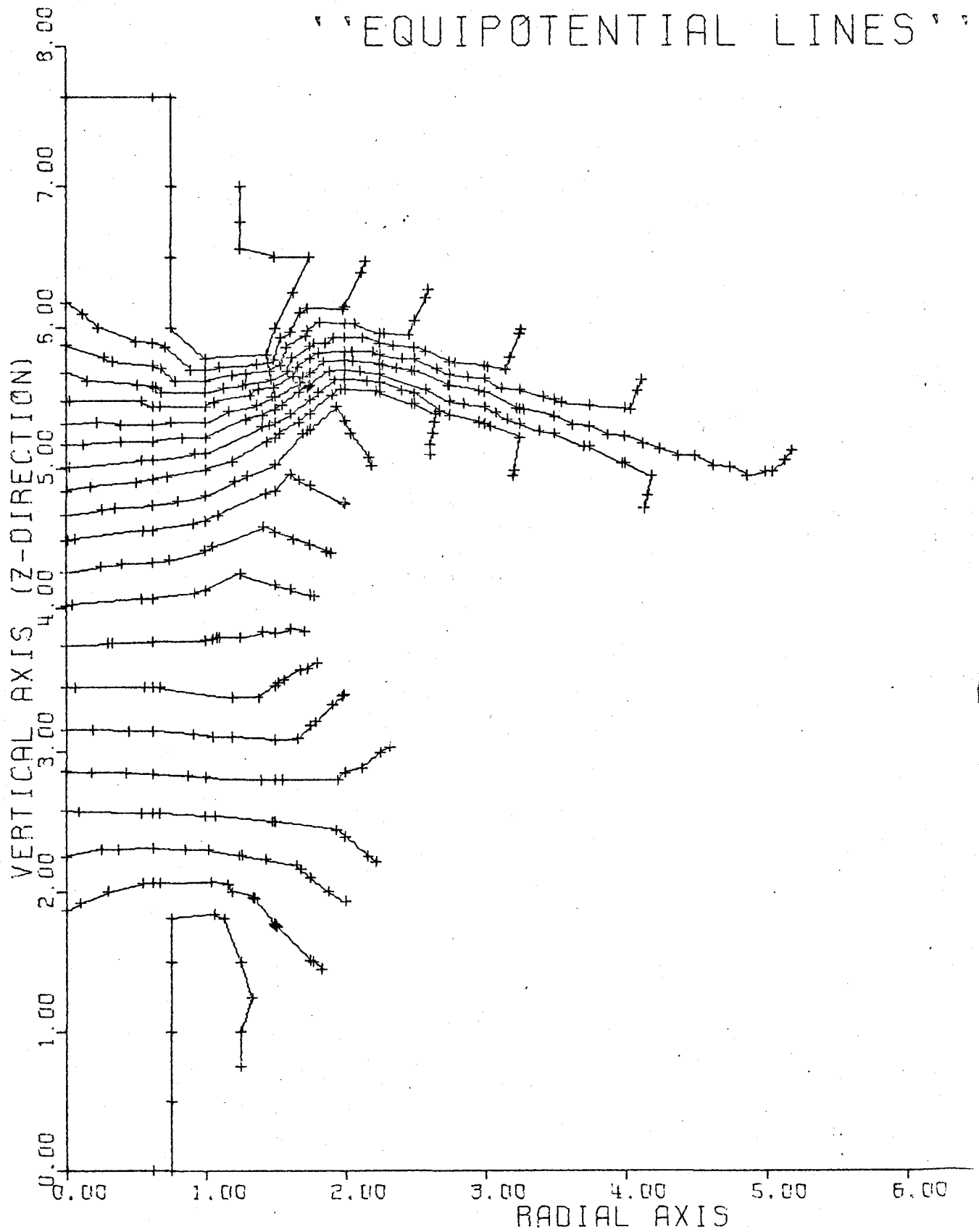


Fig. 4.7 Equipotential Lines for the Insulator

steps of five per cent of the applied voltage. Elemental electric field stress was calculated using subroutine FIELD and the highest stress was 34.0% kV r.m.s. per cm. This stress occurred in the dielectric region near the high voltage electrode shown shaded in Fig. 4.6. Although the epoxy material (dielectric strength 150 kV/cm) can withstand such a stress, if pores exist in the material, due to imperfections in casting, they might be highly stressed and may even break down. To release this stress the high voltage electrode was reshaped as shown in Fig. 4.8. The resulting maximum stress was 24.0% kV r.m.s. per cm occurring in the element shown shaded in Fig. 4.8. The corresponding equipotential lines are shown in Fig. 4.9.

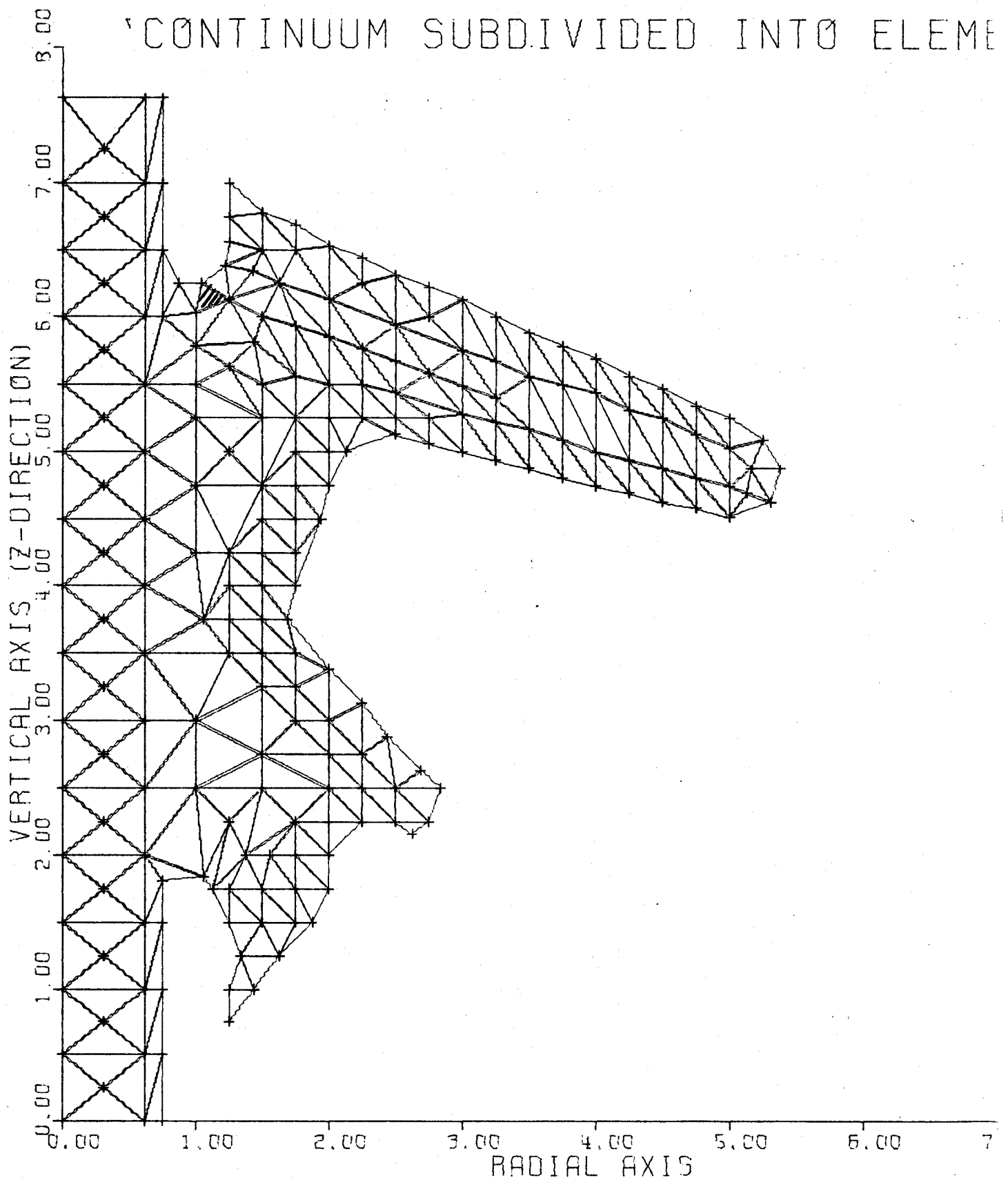


Fig. 4.8 Insulator Divided into Elements with HV Electrode Reshaped (computer plot)

1

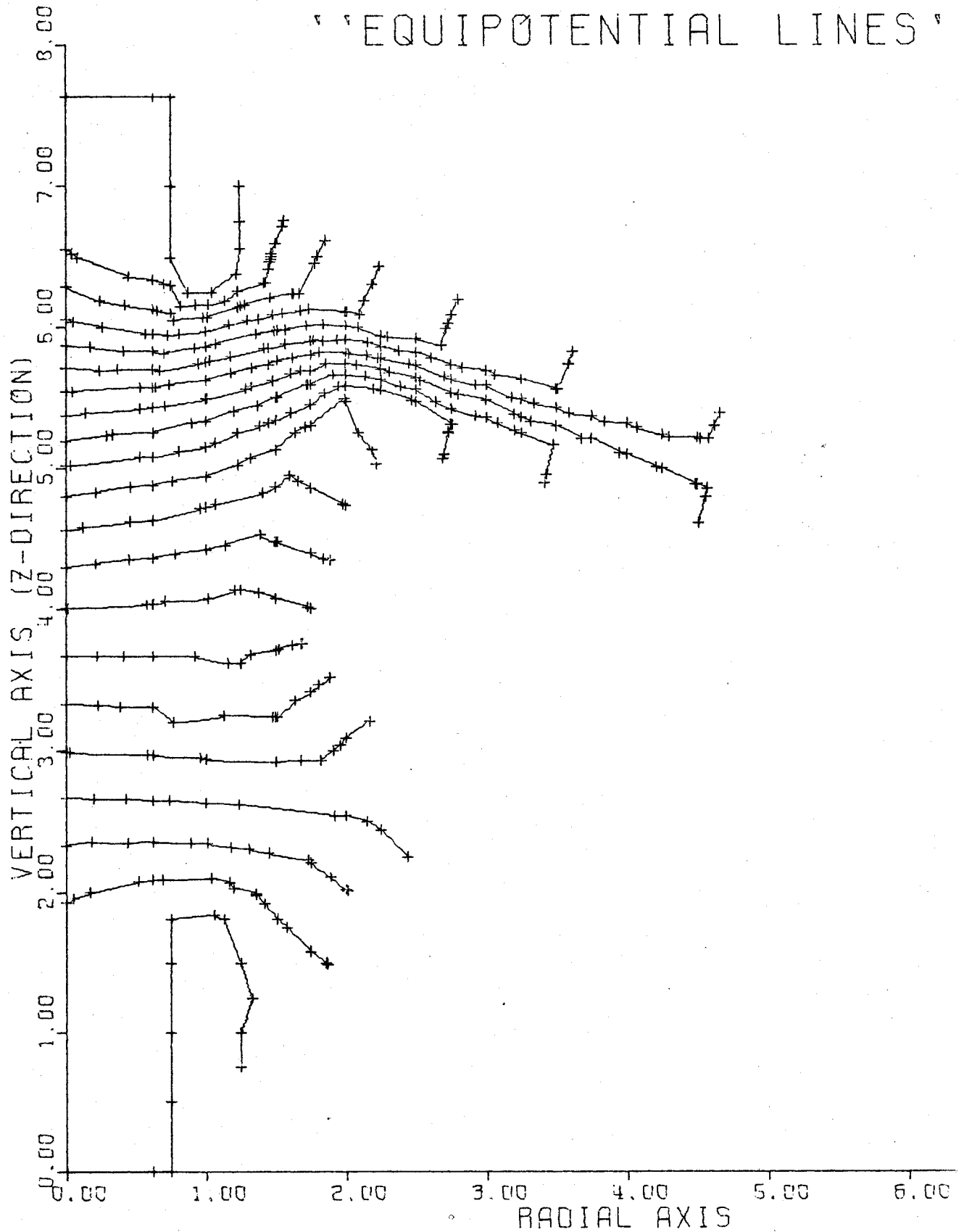


Fig. 4.9 Equipotential Lines for Insulator with Modified HV Electrodes (computer plot)

CHAPTER V

DISCUSSION AND CONCLUSION

5.1 The Numerical Methods

In both the finite difference and finite element numerical methods the error or residual between the approximate solution and the exact solution is usually a relative one. It is the difference in the value of the field function obtained at two consecutive SOR iterations for the finite difference method and the difference in the field function obtained with two consecutively decreasing element sizes or increasing order of the interpolation function in the finite element method. In the case of a frustrum with a partially-conducting outer thickness, the element size was decreased to approximately half a square centimeter and the relative error obtained for the potential function was less than one eighth of a per cent. Although this accuracy pertains mainly to the frustrum, the element size was used as a guide line when subdividing the insulator design. It should be noted that, according to the literature survey this is the first time the finite element method has been applied to calculate the field of a power line insulator.

The finite element method was found to be much superior to the finite difference method in the following respects:

- a) The finite element method requires much less time for computation than the SOR technique for a given problem. When both methods were used to compute the potential distribution in a rectangular trough, it took less than half the time with the finite element method to achieve the same accuracy as the SOR technique for an approximately equal number of nodes.
- b) For infinitely extending fields, the finite element method just requires the use of higher order interpolating functions which use more nodes per element and therefore larger element sizes. The corresponding finite difference techniques have already been given in Section 3.2.
- c) Accounting for specified boundary values of the field function at electrodes, say, is easily done by a simple program (Appendix C) in the finite element method. In the finite difference method logical commands are necessary to avoid SOR on specified boundary conditions. This has to be done during each iteration resulting in considerable computer time requirements. (Logical commands take a longer time to execute than algebraic operations).
- d) When a regular rectangular grid is used in the finite difference method, for any type of geometry mesh generation is automatically done by the computer by specifying the mesh size if different from unity in the case where more than one mesh size is used. However, in the finite element method, for complicated geometries it is difficult to generate the element pattern although nodal coordinates

may be obtained using different lines that join the nodes.

e). To improve convergence with the SOR technique requires use of an optimum convergence factor which is very difficult to determine for most practical problems. Empirical determination of the convergence factor is time consuming. Conditions used in the selection of the interpolation function in the finite element method (section 3.3.2) rigorously ensure convergence of the approximate solution to the exact solution with increasing number of elements of smaller size.²⁸

5.2 The Insulator Design

The power line-insulator designed in this work is a result of taking into consideration the various factors that lead to flashover due to pollution. Although these factors have been known for some time there is no record, from the literature survey, of an anti-pollution insulator designed in full consideration of these factors. Most designs have arisen from manufacturing technology rather than a combination of research findings and technological limitations.

The new power line-insulator design achieves the following requirements as a solution to the pollution problem affecting satisfactory operation of power line-insulators.

a) The heating effect of the current flowing in the partially-conducting material will keep the insulator surface at a temperature higher than ambient, acting as

a deterrent to moisture condensation on the insulator surface. Further, the formation of the highly stressed dry-bands that would lead to surging and possibly flash-over on the insulator surface is avoided by the partially-conducting material which offers an alternative passage of lower resistance to the leakage current. The combined effect is to decrease the chances for flashover due to pollution and the associated current surges on the insulator surface that would possibly deteriorate it.

b) Uniform voltage distribution on the surface of the new insulator avoids local stressing that would result in corona and streamer discharges. Thus in this design radio- and television-signal interference and energy losses associated with corona discharges are minimized.

c) There is considerable material saving in this design compared to deep-ribbed, corrugated anti-fog geometries.

d) The partially-conducting material has a positive temperature coefficient. There is therefore no danger of thermal runaway as exists with semi-conducting glazes.

e) The geometry of the insulator design overcomes the problem of bridging due to splashing and shed protrusion during heavy rainfall. There are no hidden areas that would accumulate windborn dirt, and the open profile facilitates ease of occasional washing of the insulator.

f) The design concept and the materials used result in relatively more compact insulators and therefore more compact transmission systems.

5.3 Suggestions for Further Work

It is now necessary to carry out artificial anti-pollution tests in the laboratory on the new insulator design. Extensive in-service tests should then be carried out. This can be done with cooperation from the Utility Company. Some units of the new insulator can be installed on spurs taken from the existing transmission lines in areas of extreme pollution; adequate switching would be installed to avoid maloperation on the main line. Such tests will result in the possibility of designing insulators for higher transmission voltages using our design concepts.

A study on installation coordination in the light of the new design should be done. Possibilities of applying our design concepts in other power line transmission hardware e.g. cross arms, apparatus insulators should be considered.

Alongside the extensive testing of the new insulator, continuum subdivision in the finite element method should be developed into a completely automatic operation for the complicated geometries of insulators. The method of boundary relaxation in the finite difference method should be developed further since most insulators have infinitely extending field distribution.

```

C
C THE FINITE DIFFERENCE METHOD
C SOLUTION OF THE EQNS. ITERATIVELY BY S.C.F.****
C
C
C FOR COMPUTER EXECUTION V(R,Z) IS REPLACED BY V(I,J)
C I FOR Z, J FOR R
C

```

```

01 DIMENSION V(50,50),X(50,50),X1(27),Y(27)
02 CALL PLOTID ('A.M.S. KATAHOIFE','U12600S170')

```

```

C
C INITIALIZATION AND ASSIGNING BOUNDARY VALUES
C

```

```

03 N=25
04 M=49
05 N1=N-1
06 M1=M-1
07 DO 1 I=1,M
08 1 V(1,I)=100.
09 V(2,I)=20.
10 V(3,I)=40.
11 V(4,I)=60.
12 V(5,I)=80.
13 DO 2 J=1,N
14 2 V(M,J)=100.
15 DO 3 J=1,N
16 3 V(1,J)=0.
17 DO 30 I=2,M1
18 DO 30 J=2,N
19 30 V(I,J)=50.
20 DO 50 J=1,N
21 50 X(1,J)=0.
22 DO 51 I=1,M
23 51 X(I,1)=0.
24 DO 52 J=1,N
25 52 X(M,J)=0.

```

```

C
C CALCULATION OF ALFOPT , THE OPTIMUM ACCELERATING FACTOR
C

```

```

26 PI=3.1415927
27 ALFOPT=2.*(1.-PI*SQRT((1./(N-1)**2)+(1./(M-1)**2)))
28 KOUNT=1
29 32 CONTINUE
30 IF(KOUNT.GE.3)ALFA=ALFOPT
31 RESMAX=0.
32 DO 9 J=2,N
33 DO 9 I=2,M1

```

```

C
C CONDITION FOR AXIS OF SYMMETRY AT J=N
C

```

```

34 IF(J.EQ.N)GO TO 7
C
C SOR GENERAL EQUATION
C

```

```

35 V(I,J)=V(I,J)+(ALFA/4.)*(V(I+1,J)+V(I-1,J)+V(I,J+1)+
36 1V(I,J-1)-4.*V(I,J))
37 GO TO 22
7 CONTINUE

```

```

C
C SOR EQUATION FOR NODES ON THE LINE OF SYMMETRY
C

```

```

38 V(I,J)=V(I,J)+(ALFA/4.)*(V(I+1,J)+V(I-1,J)+2.*V(I,J-1)
39 1-4.*V(I,J))
GO TO 4

```

```

C
C CALCULATION OF RESIDUALS AND HIGHEST VALUE STORED AS RESMAX
C

```

```

40 22 X(I,J)=V(I+1,J)+V(I-1,J)+V(I,J+1)+V(I,J-1)-4.*V(I,J)
41 GO TO 5
42 4 X(I,J)=V(I+1,J)+V(I-1,J)+2.*V(I,J-1)-4.*V(I,J)
43 5 CONTINUE
44 9 CONTINUE
45 DO 54 J=1,N
46 DO 54 I=1,M
47 IF(ABS(X(I,J)).GT.RESMAX)GO TO 53
48 GO TO 54
49 53 RESMAX=ABS(X(I,J))
50 IFSMX=I

```



```

51 JRESMX=J
52 54 CONTINUE
53 IF(KOUNT.EQ.200)GO TO 10
54 55 CONTINUE
55 KOUNT=KOUNT+1
56 GO TO 32
57 10 CONTINUE

C
C EXIT PRINT V(I,J) X(I,J) ALFOPT RESMAX
C IRESMX,JRESMX,KOUNT
C
58 WRITE(6,11) ALFOPT,RESMAX,IRESMX,JRESMX,KOUNT
59 DO 19 I=1,M
60 WRITE(6,20) (V(I,J),J=1,12)
61 19 CONTINUE
62 WRITE(6,58)
63 DO 21 I=2,M1
64 WRITE(6,20) (X(I,J),J=2,12)
65 21 CONTINUE
66 WRITE(6,58)
67 DO 33 I=1,M
68 WRITE(6,20) (V(I,J),J=13,25)
69 33 CONTINUE
70 WRITE(6,58)
71 DO 31 I=2,M1
72 WRITE(6,20) (X(I,J),J=13,25)
73 31 CONTINUE
74 11 FORMAT('0',8X,2(F8.3,8X),3I8)
75 20 FORMAT('0',13(F6.2,3X))
76 58 FORMAT('1')

C
C SORT V(I,J) AND PLOT EQUIPOTENTIAL LINES
C
77 NPTS=N+2
78 VC=90.
79 JMIN=1
80 JMAX=N
81 A=-1.0
82 300 CONTINUE
83 DO 200 J=JMIN,JMAX
84 X1(J)=FLOAT(J)/FLOAT(N)
85 I=1
86 100 I=I+1
87 IF(V(I,J).LT.VC)GO TO 100
88 Y(J)=2.*(FLOAT(I)/ELCAT(M)-((V(I,J)-VC)/(V(I,J)-
1 V(I-1,J)))/ELCAT(M))
200 CONTINUE
90 WRITE(6,58)
91 WRITE(6,400) (X1(J),Y(J),J=1,N)
92 400 FORMAT('0',2(F8.3,8X))
93 CALL CALCO2(X1,Y,27,A,4.0,8.0,0.0,0.25,0.0,0.25,+1,+1,2)
94 A=0.0
95 VC=VC-10.
96 IF(VC.GT.0.)GO TO 300
97 CALL PLTEND(4.0)
98 STOP
99 END

```

APPENDIX B

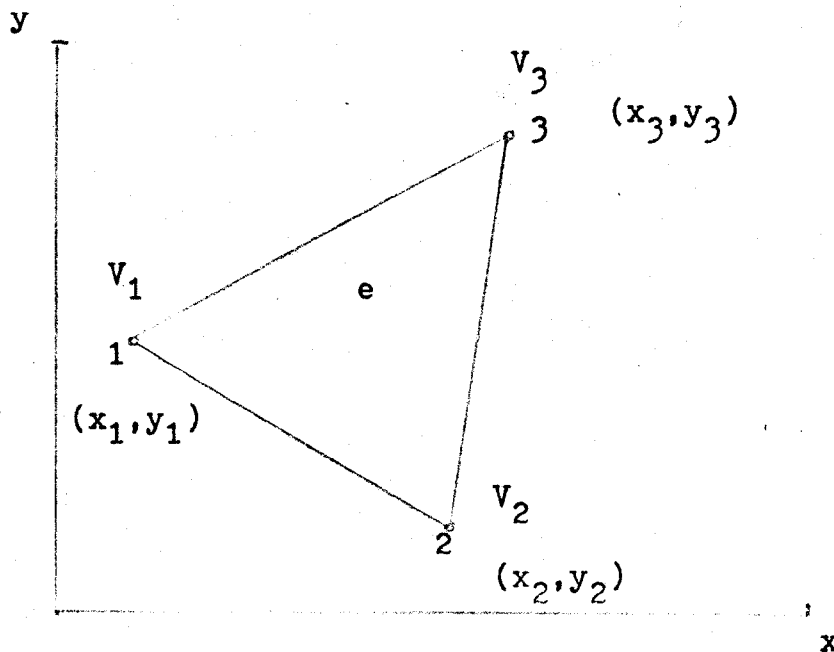


Fig. B3.7 Three node triangular Element

In Fig. B3.7 let the plane of element e be defined by the equation

$$V(x,y) = A + Bx + Cy$$

where A, B, C are constants. At each of the three nodes 1, 2, 3 $V(x,y)$ assumes the nodal values V_1, V_2, V_3 respectively, given by

$$V_1 = A + Bx_1 + Cy_1$$

$$V_2 = A + Bx_2 + Cy_2$$

$$V_3 = A + Bx_3 + Cy_3$$

$$\begin{array}{l} \text{or} \quad \begin{array}{ccc} 1 & x_1 & y_1 \\ 1 & x_2 & y_2 \\ 1 & x_3 & y_3 \end{array} \begin{array}{c} A \\ B \\ C \end{array} = \begin{array}{c} V_1 \\ V_2 \\ V_3 \end{array} \quad \text{in matrix notation} \end{array}$$

Solving for the constants A, B, C by the method of determinants gives

$$\begin{aligned} A &= \frac{\begin{vmatrix} V_1 & x_1 & y_1 \\ V_2 & x_2 & y_2 \\ V_3 & x_3 & y_3 \end{vmatrix}}{\begin{vmatrix} 1 & x_1 & y_1 \\ 1 & x_2 & y_2 \\ 1 & x_3 & y_3 \end{vmatrix}} \\ &= \frac{V_1(x_2y_3 - x_3y_2) + V_2(x_3y_1 - x_1y_3) + V_3(x_1y_2 - x_2y_1)}{2} \end{aligned}$$

$$\text{where} \quad \begin{vmatrix} 1 & x_1 & y_1 \\ 1 & x_2 & y_2 \\ 1 & x_3 & y_3 \end{vmatrix} = 2$$

= twice area of triangle e in Fig. B3.7

$$\text{Similarly } B = \frac{V_1(y_2 - y_3) + V_2(y_3 - y_1) + V_3(y_1 - y_2)}{2}$$

$$\text{and } C = \frac{V_1(x_3 - x_2) + V_2(x_1 - x_3) + V_3(x_2 - x_1)}{2}$$

Using the substitutions

$$\begin{array}{lll} a_1 = x_2y_3 - x_3y_2 & a_2 = x_3y_1 - x_1y_3 & a_3 = x_1y_2 - x_2y_1 \\ b_1 = y_2 - y_3 & b_2 = y_3 - y_1 & b_3 = y_1 - y_2 \end{array}$$

$$c_1 = x_3 - x_2$$

$$c_2 = x_1 - x_3$$

$$c_3 = x_2 - x_1$$

the expressions for A, B, C become

$$A = \frac{V_1 a_1 + V_2 a_2 + V_3 a_3}{2}$$

$$B = \frac{V_1 b_1 + V_2 b_2 + V_3 b_3}{2}$$

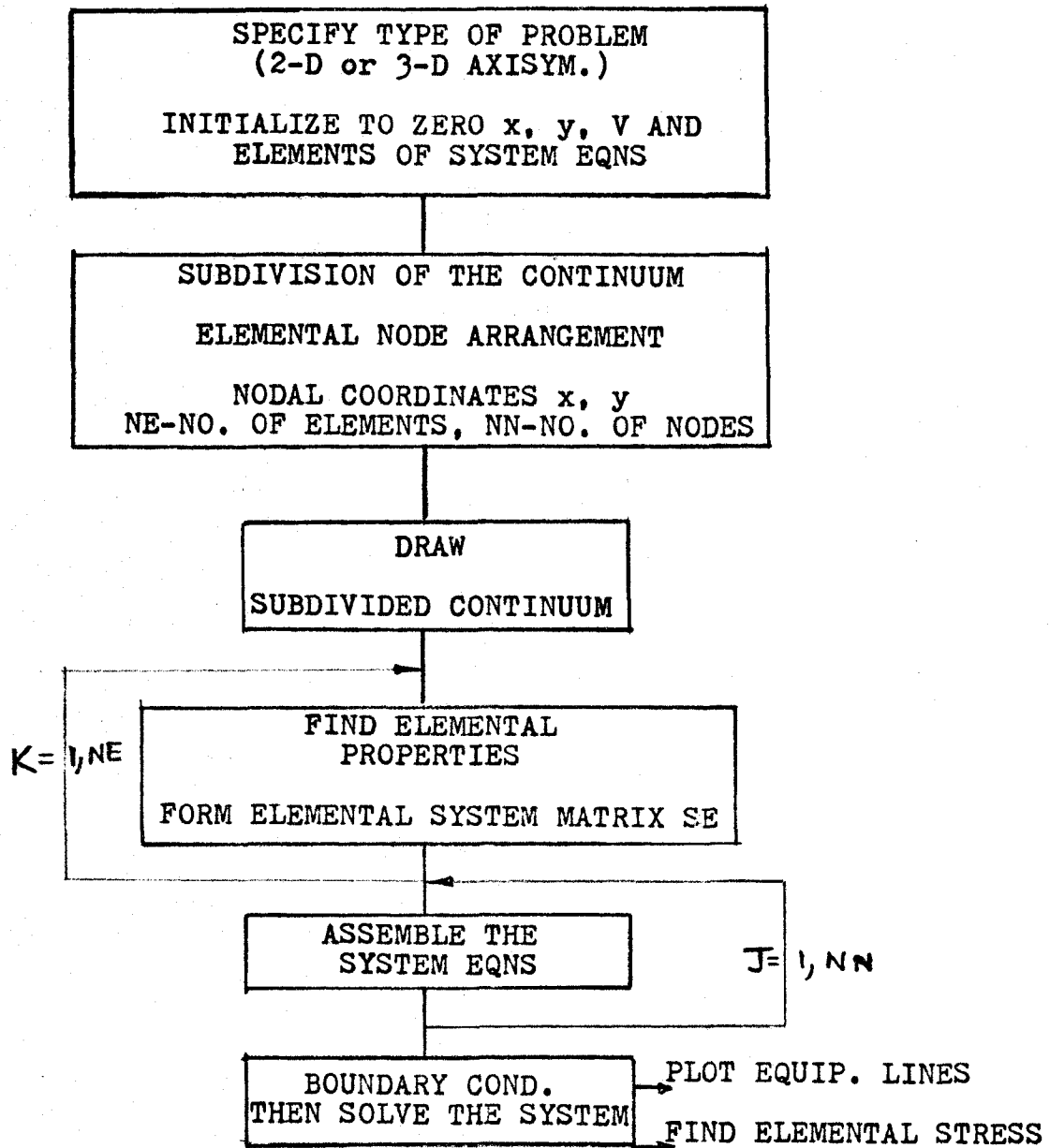
$$C = \frac{V_1 c_1 + V_2 c_2 + V_3 c_3}{2}$$

On substitution for A, B, C in the equation for V(x,y)

we get

$$V(x,y) = \frac{(a_1 + b_1 x + c_1 y) V_1 + (a_2 + b_2 x + c_2 y) V_2 + (a_3 + b_3 x + c_3 y) V_3}{2}$$

APPENDIX C



```

C**
C**THE FINITE ELEMENT METHOD
C**
1  DIMENSION X(125),Y(125),V(60),NODE(70,3)
2  DIMENSION S(52,52)
3  DIMENSION XE(3),YE(3),NC(3),SE(3,3)
C**
C**SPECIFY TYPE OF PROBLEM : 2-DIMENSION (NCASE=1)
C**OR 3-DIMENSION AXI-SYMMETRIC (NCASE=2)
C**
4  READ(5,105) NCASE
5  IF(NCASE.EQ.2) GO TO 33
6  WRITE(6,202)
7  GO TO 60
8  33 WRITE(6,303)
9  60 CONTINUE
C**
C**INITIALIZE TO ZERO S(I,J),SE(I,J),V(I),X(I),Y(I),
C**      XE(I),YE(I)
C**
10 READ(5,100) NE,NN
11 DO 2 I=1,NN
12 DO 1 J=1,NN
13 1 S(I,J)=0.0
14 X(I)=0.0
15 Y(I)=0.0
16 2 V(I)=0.0
17 DO 3 I=1,3
18 DO 3 J=1,3
19 XE(I)=0.0
20 YE(I)=0.0
21 3 SE(I,J)=0.0
C**
C**READ IN NODE NUMBERS & NODAL COORDINATES
C**
22 DO 5 K=1,NE
23 READ(5,110) NODE(K,1),NODE(K,2),NODE(K,3)
24 5 CONTINUE
25 CALL COORDS(X,Y)
C**
C**PRINT ALL THE INPUT DATA
C**
26 WRITE(6,200) NE,NN
27 DO 20 I=1,NN
28 20 WRITE(6,220) X(I),Y(I)
29 DO 25 K=1,NE
30 25 WRITE(6,240) NODE(K,1),NODE(K,2),NODE(K,3)
31 WRITE(6,210) (V(I),I=1,NN)
C**
C**DRAW THE SUBDIVIDED CONTINUUM BY SUBROUTINE ELMNTS
C**
32 CALL ELMNTS(NE,X,Y,NODE)
C**
C**FIND ELEMENTAL PROPERTIES
C**
33 DO 35 K=1,NE
34 N1=NODE(K,1)
35 N2=NODE(K,2)
36 N3=NODE(K,3)
C**
37 XE(1)=X(NODE(K,1))
38 XE(2)=X(NODE(K,2))
39 XE(3)=X(NODE(K,3))
C**
40 YE(1)=Y(NODE(K,1))
41 YE(2)=Y(NODE(K,2))
42 YE(3)=Y(NODE(K,3))
C**
43 E1=YE(3)-YE(2)
44 E2=YE(1)-YE(3)
45 E3=YE(2)-YE(1)
C**
46 C1=XE(2)-XE(3)
47 C2=XE(3)-XE(1)
48 C3=XE(1)-XE(2)
49 DEL=ABS(.5*(XE(1)*(YE(2)-YE(3))+XE(2)*(YE(3)-YE(1))
50 1+XE(3)*(YE(1)-YE(2))))
51 PI=3.14159
RBAR=(XE(1)+XE(2)+XE(3))/3.0

```

```

52      AA=1.0
53      IF(NCASE.EQ.2)AA=2.*PI*RBAR**2
54      CONST=AA/(4.*DEL)
55      SE(1,1)=(B1*B1+C1*C1)*CCNST
56      SE(1,2)=(B1*B2+C1*C2)*CCNST
57      SE(1,3)=(B1*B3+C1*C3)*CCNST
58      SE(2,1)=SE(1,2)
59      SE(2,2)=(B2*B2+C2*C2)*CCNST
60      SE(2,3)=(B2*B3+C2*C3)*CCNST
61      SE(3,1)=SE(1,3)
62      SE(3,2)=SE(2,3)
63      SE(3,3)=(B3*B3+C3*C3)*CCNST

C**
C**ASSEMBLE SYSTEM EQUATIONS WITHOUT BOUNDARY CCNDITIONS
C**

64      NO(1)=N1
65      NO(2)=N2
66      NO(3)=N3
67      DO 30 IE=1,3
68      I=NO(IE)
69      DO 30 JE=1,3
70      J=NO(JE)
71      S(I,J)=S(I,J)+SE(IE,JE)
72      30 CONTINUE

C**
C**RECYCLE FOR NEXT ELEMENT
C**

73      35 CONTINUE

C**
C**ACCCUNT FOR SPECIFIED BOUNDARY CCNDITIONS
C**

74      DO 40 I=1,18,17
75      V(I)=100.0
76      DO 40 J=1,NN
77      IF(I.NE.J)GO TO 36
78      GO TO 37
79      36 CONTINUE
80      V(J)=V(J)-V(J)*S(I,J)
81      S(I,J)=0.0
82      GO TO 40
83      37 CONTINUE
84      S(I,J)=1.0
85      40 CONTINUE
86      DO 45 I=23,36,13
87      V(I)=100.0
88      DO 45 J=1,NN
89      IF(I.NE.J)GO TO 41
90      GO TO 42
91      41 CONTINUE
92      V(J)=V(J)-V(J)*S(I,J)
93      S(I,J)=0.0
94      GO TO 45
95      42 CONTINUE
96      S(I,J)=1.0
97      45 CONTINUE

C**
98      DO 50 I=17,52,35
99      V(I)=0.0
100     DO 50 J=1,NN
101     IF(I.NE.J)GO TO 46
102     GO TO 47
103     46 CONTINUE
104     V(J)=V(J)-V(J)*S(I,J)
105     S(I,J)=0.0
106     GO TO 50
107     47 CONTINUE
108     S(I,J)=1.0
109     50 CONTINUE

C**
C**SOLVE THE SYSTEM EQUATIONS BY SUBROUTINE SIMQ
C**

110     KS=1
111     NA=NN*NN
112     CALL SIMQ(S,V,NN,NA,KS)
113     DO 65 I=1,NN
114     WRITE(6,260)V(I)
115     65 CONTINUE

C**
C**PLOT THE EQUIPOTENTIAL LINES BY SUBROUTINE CCNTUA
C**

```

```

116      CALL CONTUA(NE,V,NODE,X,Y)
C**
C**MAKE ADDITIONAL COMPUTATIONS:FIND THE ELEMENTAL
C** ELECTRIC STRESS BY SUBROUTINE FIELD
C**
117      CALL FIELD(X,Y,V,NE,NCASE,NODE)
C**
C**FORMATS : READ 100 TO 190 ,WRITE 200 TO 280
C**
118      100 FORMAT(2I4)
119      105 FORMAT(I2)
120      110 FORMAT(3I4)
C**
121      200 FORMAT(8X,2(I4,8X))
122      202 FORMAT('C',16X,'THIS IS A TWO-DIMENSIONAL PROBLEM')
123      210 FORMAT('C',12F9.4)
124      220 FORMAT('C',8X,2(F8.5,8X))
125      240 FORMAT('C',8X,3(I4,8X))
126      260 FORMAT('C',16X,F8.4)
127      303 FORMAT('C',16X,'THIS IS A THREE-DIMENSIONAL
1AXI-SYMMETRIC PROBLEM')
128      STOP
129      END

```

```

130      SUBROUTINE ELMNTS(NE,X,Y,NODE)
131      DIMENSION X(125),Y(125),NCDE(200,3),XP(6),YP(6)
132      NPTS=6
133      A=-1.0
134      DO 1 K=1,NE
135      DO 2 I=1,3
136      XP(I)=X(NCDE(K,I))
137      2 YP(I)=Y(NCDE(K,I))
138      YP(4)=YP(1)
139      XP(4)=XP(1)
140      CALL CALCC2(XP,YP,NPTS,A,4.0,8.0,C.0,-C.25,C.0,C.25,+1,-1.2)
141      A=.0
142      1 CONTINUE
143      RETURN
144      END

```



```
145 SUBROUTINE FIELD(X,Y,V,NE,NCASE,NCDE)
146 DIMENSION X(125),Y(125),V(60),STRESS(70),NCDE(70,3)
147 PI=3.14159
148 DO 10 K=1,NE
149 X1=X(NCDE(K,1))
150 X2=X(NCDE(K,2))
151 X3=X(NCDE(K,3))
152 Y1=Y(NCDE(K,1))
153 Y2=Y(NCDE(K,2))
154 Y3=Y(NCDE(K,3))
      C***
155 B1=Y3-Y2
156 B2=Y1-Y3
157 B3=Y2-Y1
      C***
158 C1=X2-X3
159 C2=X3-X1
160 C3=X1-X2
      C***
161 V1=V(NCDE(K,1))
162 V2=V(NCDE(K,2))
163 V3=V(NCDE(K,3))
      C***
164 RBAR=(X1+X2+X3)/3.0
165 AA=1.0
166 AREA=ABS(0.5*(X1*(Y2-Y3)+X2*(Y3-Y1)+X3*(Y1-Y2)))
167 CONST=AA/(2.0*AREA)
168 GRADX=(B1*V1+B2*V2+B3*V3)*CONST
169 GRADY=(C1*V1+C2*V2+C3*V3)*CONST
170 STRESS(K)=SQRT(GRADX**2+GRADY**2)
171 WRITE(6,200) K,STRESS(K)
172 10 CONTINUE
173 200 FORMAT('0', 'THE STRESS IN ELEMENT', I4, '= ', F8.4)
174 RETURN
175 END
```

```
176 SUBROUTINE CONTUA(NE,V,NODE,X,Y)
177 DIMENSION NODE(70,3),V(60),Y(125),X(125),XP(100),YP(100)
178 200 FORMAT('0',8X,2F16.5)
179 J=1
180 VC=100.0
181 10 CONTINUE
182 NPTS=2
183 L=0
184 DO 7 K=1,NE
185 X1=X(NODE(K,1))
186 X2=X(NODE(K,2))
187 X3=X(NODE(K,3))
188 Y1=Y(NODE(K,1))
189 Y2=Y(NODE(K,2))
190 Y3=Y(NODE(K,3))
191 V1=V(NODE(K,1))
192 V2=V(NODE(K,2))
193 V3=V(NODE(K,3))
C ***
194 IF(V1.EQ.V2)GO TO 3
195 IF(V1.GE.VC.AND.VC.GE.V2)GO TO 2
196 IF(V1.LE.VC.AND.VC.LE.V2)GO TO 2
197 GO TO 3
198 2 CONTINUE
199 L=L+1
200 YP(L)=(X2*(V1-V2)+(VC-V2)*(X1-X2))/(V1-V2)
201 XP(L)=(Y2*(V1-V2)+(VC-V2)*(Y1-Y2))/(V1-V2)
202 3 CONTINUE
203 IF(V2.EQ.V3)GO TO 5
204 IF(V2.GE.VC.AND.VC.GE.V3)GO TO 4
205 IF(V2.LE.VC.AND.VC.LE.V3)GO TO 4
206 GO TO 5
207 4 CONTINUE
208 L=L+1
209 YP(L)=(X3*(V2-V3)+(VC-V3)*(X2-X3))/(V2-V3)
210 XP(L)=(Y3*(V2-V3)+(VC-V3)*(Y2-Y3))/(V2-V3)
211 5 CONTINUE
212 IF(V1.EQ.V3)GO TO 7
213 IF(V1.GE.VC.AND.VC.GE.V3)GO TO 6
214 IF(V1.LE.VC.AND.VC.LE.V3)GO TO 6
215 GO TO 7
216 6 CONTINUE
217 L=L+1
218 YP(L)=(X3*(V1-V3)+(VC-V3)*(X1-X3))/(V1-V3)
219 XP(L)=(Y3*(V1-V3)+(VC-V3)*(Y1-Y3))/(V1-V3)
220 7 CONTINUE
221 NPTS=NPTS+L
222 IF(NPTS.LT.4)GO TO 8
223 WRITE(6,200)VC
224 CALL SORT(XP,YP,L)
225 8 CONTINUE
226 J=J+1
227 VC=VC-5.0
228 A=0.0
229 IF(VC.GE.0.0)GO TO 10
230 RETURN
231 END
```

```
232 SUBROUTINE SORT(XP,YP,L)
233 DIMENSION XP(100),YP(100)
234 200 FORMAT('C',8X,2F16.5)
235 L1=L-1
236 DO 2 I=1,L
237 K=I
238 IF(K.EQ.L) GO TO 2
239 DO 3 J=K,L1
240 IF(YP(I).LE.YP(J+1))GO TO 3
241 YTEMP=YP(I)
242 YP(I)=YP(J+1)
243 YP(J+1)=YTEMP
244 XTEMP=XP(I)
245 XP(I)=XP(J+1)
246 XP(J+1)=XTEMP
247 3 CONTINUE
248 2 CONTINUE
249 WRITE(6,200) (YP(J),XP(J),J=1,L)
250 RETURN
251 END
```

APPENDIX D

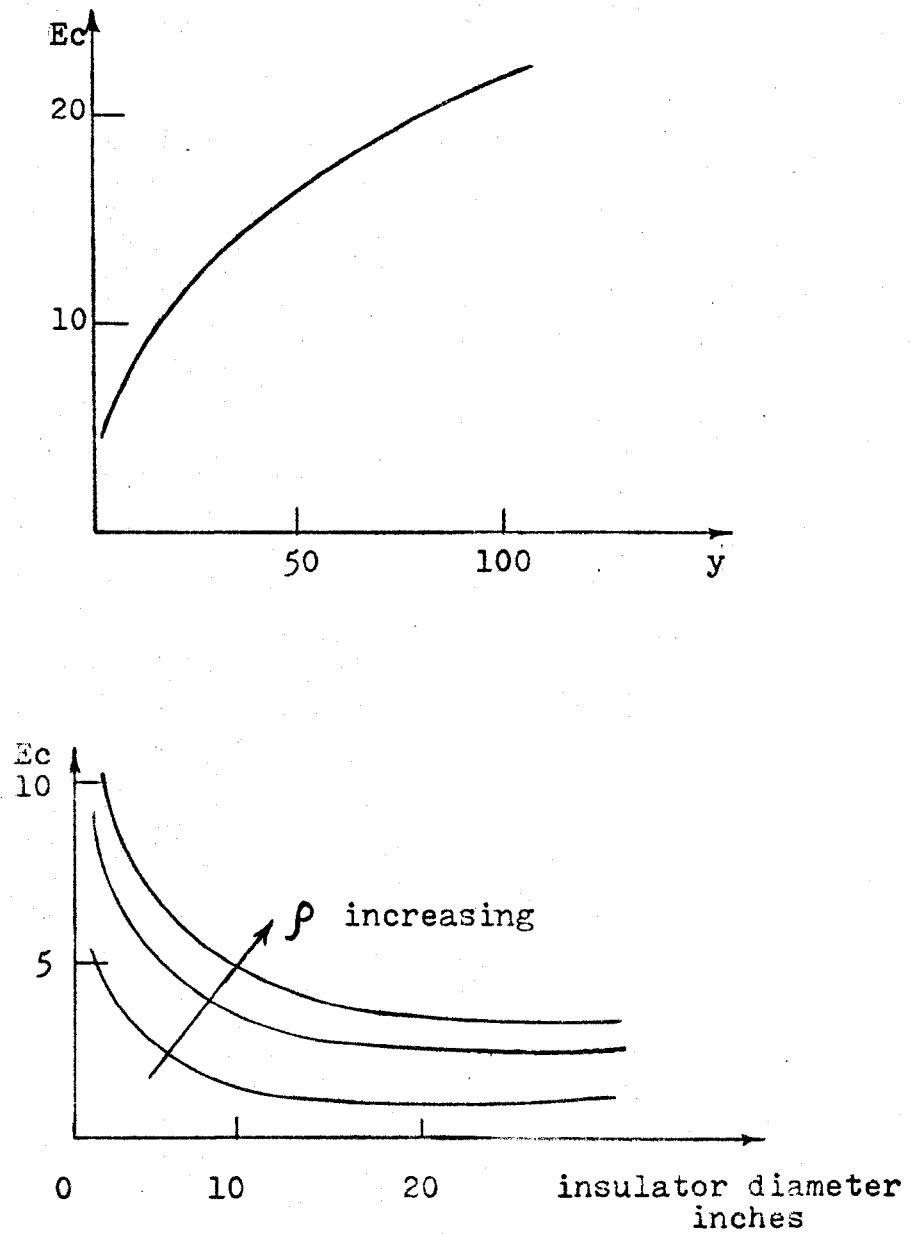


Fig. D 2.1 The Effect of y , number of discharges, insulator diameter on E_c ¹²

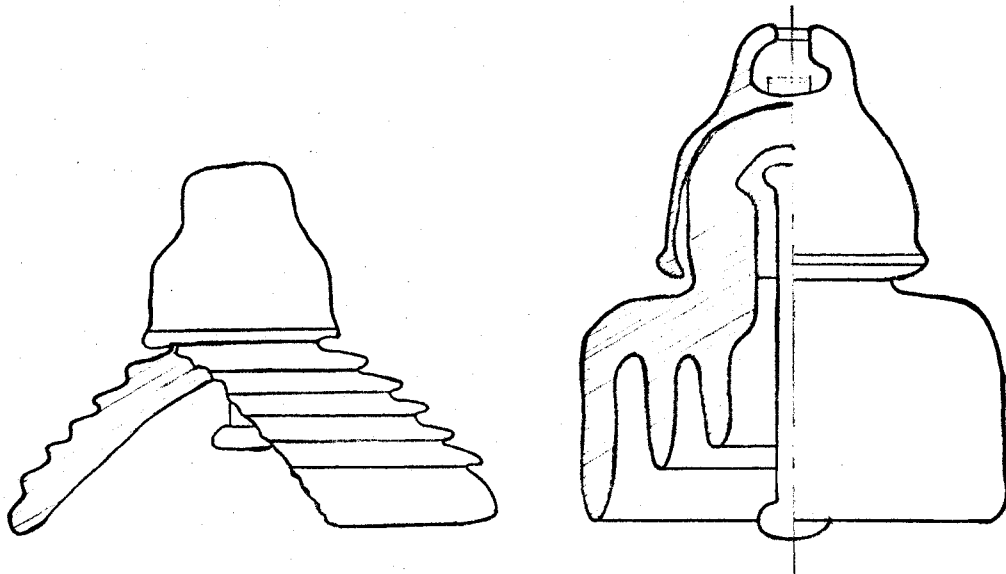
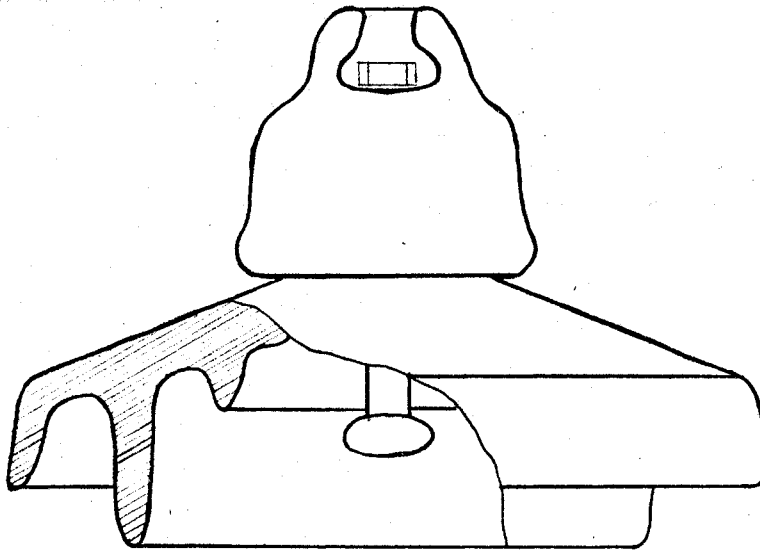


Fig. D 2.2 Conventional Anti-Fog Insulators 33

BIBLIOGRAPHY

1. Knowlton, A.E., 'Standard Handbook for Electrical Engineers'. McGraw-Hill, New York, 1959.
2. Cotton, H. and Barber, H., 'The Transmission and Distribution of Electrical Energy'. The English Universities Press, London, 1970.
3. Peaslee, W.D.R., 'Factors Controlling the Design and Selection of Suspension Insulators'. Trans. A.I.E.E., Vol. 39, Part II, 1920. pp. 1645-1667.
4. Hawley, K.A., 'Development of the Porcelain Insulator'. Trans. A.I.E.E., Vol. 50, 1, 1931 pp. 47-54.
5. Skowronski, J.I., Pohl, Z., 'The Effect of the Type of Pollution on the Selection of the Shape of Outdoor Insulators and Testings'. CIGRE, 1968, 22nd Session, Vol. I Paper 25-07 pp. 1-6.
6. Rizk, A.M. El-Sarky, A., Assaad, A.A., Amad, M.M., 'Comparative Tests on Contaminated Insulators with reference to Desert Conditions'. CIGRE, 1972, 24th Session, Vol. II Paper 33-03 pp. 1-9.
7. John, W.J., Clark, C.W., 'Testing of Transmission-line Insulators under Deposit Conditions'. Proc. I.E.E., Vol. 85, 1939, pp. 590-624.
8. Scott-Maxwell, I.S., 'Suspension Insulators for E.H.T. Transmission'. Proc. I.E.E., Vol. 79, 1936, pp. 236-237.
9. Lambeth, P.J., Looms, J.S.T., Stalewski, A., Todd, W.G., 'Surface Coatings for H.V. Insulators in Polluted Areas'. Proc. I.E.E., Vol. 113, 5, May 1966, pp. 861-869.
10. Johnson, J., Henderson, R.T., Price, W.S., Hedman, D.E., Turner, F.J., 'Field and Laboratory Tests of Contaminated Insulators for the Design of the State Electricity Commission of Victoria's 500 kV System'. Trans. I.E.E.E., Vol. PAS-87, 5, 1968, pp. 1216-1239.
11. Hampton, B.F., 'Flashover Mechanism of Polluted Insulation'. Proc. I.E.E., Vol. III, 5, May 1964, pp. 985-990.
12. Billings, M.J., Wilkins, R., 'Considerations of the Suppression of Insulator Flashover by Resistive Surface Films'. Proc. I.E.E., Vol. 113, 10, 1966, pp. 1649-1653.

13. Udo, T., 'Switching Surge Sparkover Characteristics of Air Gaps and Insulator Strings under Practical Conditions'. Trans. I.E.E.E., Vol. PAS-85, 8, May 1966, pp. 859-864.
14. Hirose, Y., Seta, T., 'Switching Surge Insulation Characteristics of Insulators under Polluted Conditions'. CIGRE, 1972, 24th Session, Vol. II Paper 33-02 pp. 1-8.
15. Gillam, G.H. CIGRE Progress Report of Study Committee on Insulators, 1968, 22nd Session, Vol. II Paper 25-01.
16. Lambeth, P.J., and Looms, J.S.T., (U.K.), Sforzin, M., and Malaguti, C., (Italy), Porcheron, Y., and Claverie, P., (France), 'International Research on Polluted Insulators'. CIGRE, 1970, 23rd Session, Paper 33-02 pp. 1-16.
17. Fukui, H., Naito, K., Irie, T., Kimoto, I., 'A Practical Study of Semiconducting Glaze Insulators to Transmission Lines'. I.E.E.E., Paper 74 073-3, Winter Meeting, 1974, New York, pp. 1430-1443.
18. Moran, J.H., Powell, D.G., 'Resistance Graded Insulators -- The Ultimate Solution to the Contamination Problem?'. I.E.E.E., Paper T 72 202-5, Winter Meeting, 1972, New York, pp. 2452-2458.
19. Robinson, W.G., 'Developments in Porcelain Insulators'. Electrical Review (G.B.), Vol. 191, 14, Oct. 1972, pp. 435-438.
20. Vitkovitch, D., 'Field Analysis'. D. Van Nostrand, London, 1966.
21. Binns, K.J., Lawrenson, P.J., 'Analysis and Computation of Electric and Magnetic Field Problems'. Macmillan, New York, 1963.
22. Storey, J.T., Billings, M.J., 'General Digital-Computer Program for the Determination of Three-Dimensional Electrostatic Axially Symmetric Fields'. Proc. I.E.E.E., Vol. 114, 10, Oct. 1967, pp. 1551-1555.
23. Frankel, S.P., 'Convergence Rates of Iterative Treatments of Partial Differential Equations'. Math. Tab., Wash. Vol. IV, 30, April 1950, pp. 65-75.
24. Wensley, B.A., Parker, F.W., 'The Solution of Electric Field Problems Using a Digital Computer'. Electrical Energy, 1960, pp. 12-16.

25. Sandy, F., Sage, J., 'Use of Finite Difference Approximations for Problems Having Boundaries at Infinity'. Trans. I.E.E.E., Vol. MTT-19, 5, 1971, pp. 484-486.
26. Desai, C.S., Abel, J.F., 'Introduction to the Finite Element Method'. V. Nostrand Reinhold, New York, 1972.
27. Huebner, K.H., 'The Finite Element Method for Engineers'. Wiley, New York, 1975.
28. Zienkiewicz, O.C., 'The Finite Element Method in Engineering Science'. McGraw-Hill, London, 1971.
29. Norrie, D.H., de Vries, G., 'The Finite Element Method'. Academic Press, New York, 1973.
30. Sangha, S.S., 'Development of Materials for EHV and UHV Insulation Operated in Polluted Environment'. M.A.Sc. Thesis Oct. 1975, University of Windsor.
31. Forrest, J.S., 'The Electrical Characteristics of 132 kV Line Insulators under Various Weather Conditions'. Proc. I.E.E.E., Vol. 79, 1936, p. 402.
32. John, W.J., Sayers, F.M., 'Transmission-line Insulators under Deposit Conditions'. Proc. I.E.E.E., Vol. 79, 1936, pp. 629-662.
33. Ranachowski, J., Winkler, J., 'Choice of the Shape of Epoxy Resin Insulators'. Przegląd Elechtroch. (Poland), Vol. 42, 6, June 1966, pp. 230-233.
34. Pohl, Z., 'High-Voltage Insulation under Polluted Conditions'. Scientific Papers of the Institute of Electrical Engineering Fundamentals of Wroclaw Technical University, No. 10, Monograph No. 4, 1975.
35. Robinson, W.G., 'Extra-High-Voltage Insulators'. Electrical Review, Vol. I, January 1960, pp. 3-6.

VITA AUCTORIS

A.M S. KATAHOIRE

- 1950 Born 25th May in Hoima, Uganda.
- 1970 Completed East African Advanced Certificate of Education at Makerere College School, Kampala, Uganda.
- 1974 Graduated B.Sc. (Elect. Engg.) (Hons.) from The University of Nairobi, Nairobi, Kenya.
- 1974 Worked as Electrical Design Engineer with the National Housing and Construction Corporation, Kampala, Uganda.
- 1976 Candidate for the Degree of M.A.Sc., Electrical Engineering, University of Windsor, Windsor, . Ontario, Canada.